Table 2 ^{1}H and ^{13}C NMR data (500 and 125 MHz) for compounds **5** and **6**

Positions	**5**[a]		Positions	**6**[b]	
	δ_H (*J* Hz)	δ_C		δ_H (*J* Hz)	δ_C
1		126.4	1		108.3
2	7.46 (1H, d, 2.0)	111.6	2		161.9
3		147.7	3	6.40 (1H, d, 2.3)	95.8
4		152.6	4		164.7
5	6.85 (1H, d, 8.3)	115.2	5	6.24 (1H, d, 2.3)	99.1
6	7.50 (1H, dd, 2.0, 8.3)	123.2	6		167.0
7		193.9	7		205.4
8	4.77, 4.91 (1H each, both d, 15.8)	70.7	8	2.71 (3H, s)	33.7
3-OCH_3	3.82 (3H, s)	55.8			
Glc-1′	4.31 (1H, d, 7.7)	102.7	Glc-1′	5.09 (1H, d, 7.8)	101.6
Glc-2′	3.07 (1H, dd, 7.7, 8.3)	73.4	Glc-2′	3.51 (1H, m)	74.6
Glc-3′	3.18 (1H, dd, 8.3, 9.2)	76.7	Glc-3′	3.51 (1H, m)	78.7
Glc-4′	3.04 (1H, dd, 8.9, 9.2)	70.2	Glc-4′	3.36 (1H, m)	71.4
Glc-5′	3.31 (1H, ddd, 1.7, 6.5, 8.9)	75.8	Glc-5′	3.72 (1H, m)	77.1
Glc-6′	3.45 (1H, m)	67.2	Glc-6′	3.58 (1H, m)	68.8
	3.82 (1H, dd, 1.7, 11.5)			4.05 (1H, dd, 1.8, 11.2)	
Rha-1″	4.61 (1H, d, 1.4)	101.0	Api-1″	4.96 (1H, d, 2.6)	110.9
Rha-2″	3.64 (1H, dd, 1.4, 3.5)	70.6	Api-2″	3.96 (1H, d, 2.6)	77.9
Rha-3″	3.43 (1H, m)	70.8	Api-3″		80.5
Rha-4″	3.19 (1H, dd, 2.3, 9.5)	72.1	Api-4″	3.75, 3.97 (1H each, both d, 9.8)	75.0
Rha-5″	3.46 (1H, m)	68.5	Api-5″	3.58 (2H, m)	65.5
Rha-6″	1.12 (3H, d, 6.0)	18.0			
			Glc-1‴	5.05 (1H, d, 7.5)	100.8
			Glc-2‴	3.51 (1H, m)	74.6
			Glc-3‴	3.51 (1H, m)	78.3
			Glc-4‴	3.36 (1H, m)	71.6
			Glc-5‴	3.51 (1H, m)	77.9
			Glc-6‴	3.70 (1H, m)	62.5
				3.91 (1H, dd, 2.0, 12.0)	

[a] Measured in DMSO-d_6

[b] Measured in CD_3OD

Thus, a long-range correlation was observed between the anomeric proton of the β-D-apiofuranosyl group (1″-H) and the 6′-carbon in the 2-*O*-β-D-glucopyranosyl group (δ_C 68.8) as shown in Fig. 2. On the basis of the above-mentioned evidence, the structure of kaempferiaoside F was determined to be 2,4,6-trihydroxyacetophenone 2-*O*-β-D-apiofuranosyl-(1→6)-β-D-glucopyranosyl 4-*O*-β-D-glucopyranoside (**6**).

Experimental method

General

The following instruments were used to obtain spectroscopic data: specific rotations, Horiba SEPA-300 digital polarimeter (l = 5 cm); CD spectra, Jasco J-720WI spectrometer; UV spectra, Shimadzu UV-1600 spectrometer; IR spectra, Shimadzu FTIR-8100 spectrometer; FAB-MS and high-resolution MS, JEOL JMS-SX 102A mass spectrometer; ^{1}H-NMR spectra, JEOL JNM-ECA700 (700 MHz) and JNM-ECA500 (500 MHz) spectrometers; ^{13}C-NMR spectra, JEOL JNM-ECA700 (175 MHz) and JNM-ECA500 (125 MHz) spectrometers with tetramethylsilane as an internal standard; and HPLC detector, Shimadzu SPD-10A*vp* UV–VIS detector; HPLC column, Cosmosil 5C_{18}-MS-II and πNAP (250 × 4.6 mm i.d. and 250 × 20 mm i.d. for analytical and preparative purposes, respectively).

The following experimental conditions were used for chromatography (CC): ordinary-phase silica gel column chromatography, silica gel 60 N (Kanto Chemical Co., Tokyo, Japan; 63–210 mesh, spherical, neutral); reverse-phase silica gel CC, Diaion HP-20 (Nippon Rensui, Tokyo, Japan) and Chromatorex ODS DM1020T (Fuji Silysia Chemical, Aichi, Japan; 100–200 mesh); normal-phase

TLC, pre-coated TLC plates with silica gel $60F_{254}$ (Merck, Darmstadt, Germany; 0.25 mm); reversed-phase TLC, pre-coated TLC plates with silica gel RP-18 F_{254S} (Merck, 0.25 mm); reversed-phase HPTLC, pre-coated TLC plates with silica gel RP-18 WF_{254S} (Merck, 0.25 mm), detection was achieved by spraying with 1% $Ce(SO_4)_2$–10% aqueous H_2SO_4, followed by heating.

Plant material

The rhizomes of *Kaempferia parviflora* Wall. ex Baker cultivated at Loei province, Thailand, were purchased from a traditional drug store in Nakhonsithammarat province, Thailand, on May 2008. The plant material was identified by one of the authors (Y. P.). A voucher specimen (2008.05. Raj-03) of this plant is on file in our laboratory, as described in a previous report [19].

Extraction and isolation

The dried rhizomes of *K. parviflora* (1.8 kg) were finely cut and extracted four times with MeOH under reflux for 4 h. Evaporation of the combined extracts under reduced pressure provided a MeOH extract (128.0 g, 7.10%). An aliquot (108.0 g) was partitioned into an EtOAc–H_2O (1:1, v/v) mixture to furnish an EtOAc-soluble fraction (58.10 g, 3.82%) and an aqueous phase. The aqueous phase was subjected to Diaion HP-20 CC (1.5 kg, H_2O → MeOH) to give H_2O-eluted (30.98 g, 2.04%) and MeOH-eluted (18.66 g, 1.23%) fractions, as described previously [19]. The MeOH-eluted fraction (13.60 g) was subjected to normal-phase silica gel CC [600 g, $CHCl_3$–MeOH–H_2O (10:3:0.4 → 7:3:0.5 → 6:4:1, v/v/v) → MeOH → acetone] to give 10 fractions [Fr. 1 (1113.3 mg), Fr. 2 (588.8 mg), Fr. 3 (606.2 mg), Fr. 4 (268.0 mg), Fr. 5 (519.8 mg), Fr. 6 (985.6 mg), Fr. 7 (634.1 mg), Fr. 8 (1850.0 mg), Fr. 9 (3.50 g), and Fr. 10 (3.50 g)]. Fraction 3 (606.2 mg) was subjected to reversed-phase silica gel CC [19 g, MeOH–H_2O (20:80 → 50:50 → 70:30, v/v) → MeOH] to afford six fractions [Fr. 3-1 (97.7 mg), Fr. 3-2 (97.3 mg), Fr. 3-3 (155.6 mg), Fr. 3-4 (137.1 mg), Fr. 3-5 (11.5 mg), and Fr. 3-6 (16.6 mg)], as described previously [19]. Fraction 3-2 (97.3 mg) was purified by HPLC [Cosmosil $5C_{18}$-MS-II, MeOH–1% aqueous AcOH (15:85, v/v)] to give kaempferiaoside E (**5**, 24.8 mg, 0.0022%). Fraction 3-3 (155.6 mg) was separated by HPLC [Cosmosil $5C_{18}$-MS-II, MeOH–1% aqueous AcOH (15:85, v/v)] to give **3** (7.1 mg, 0.00060%) together with L-phenylalanine (7.4 mg, 0.00070%). Fraction 6 (985.6 mg) was subjected to reversed-phase silica gel CC [30 g, MeOH–H_2O (10:90 → 20:80 → 50:50, v/v) → MeOH] to afford eight fractions [Fr. 6-1 (41.6 mg), Fr. 6-2 (33.6 mg), Fr. 6-3 (127.1 mg), Fr. 6-4 (98.9 mg), Fr. 6-5 (44.7 mg), Fr. 6-6 (30.1 mg), Fr. 6-7 (51.3 mg), and Fr. 6-8 (327.0 mg)], as described previously [19]. Fraction 6-3 (127.1 mg) was separated by HPLC [Cosmosil $5C_{18}$-MS-II, MeOH–1% aqueous AcOH (10:90, v/v)] to give kaempferiaoside F (**6**, 16.1 mg, 0.0015%) together with 2,4,6-trihydroxyacetophenone-2,4-di-*O*-β-D-glucopyranoside (4.7 mg, 0.00043%). Fraction 6-4 (98.9 mg) was purified by HPLC [Cosmosil $5C_{18}$-MS-II, MeOH–1% aqueous AcOH (20:80, v/v)] to give kaempferiaosides C (**3**, 5.5 mg, 0.00050%) and D (**4**, 3.2 mg, 0.00030%) together with *rel*-(5a*S*,10b*S*)-5a,10b-dihydro-1,3,5a,9-tetrahydroxy-8-methoxy-6*H*-benz[*b*]indeno[1,2-*d*]furan-6-one 5a-*O*-[α-L-rhamnopyranosyl-(1→6)-β-D-glucopyranoside] (26.6 mg, 0.0024%).

Kaempferiaoside C (3)

Amorphous powder, $[\alpha]_D^{23}$ −65.6° (*c* 0.24, MeOH). CD [MeOH, nm (Δε)]: 224 (−7.92), 244 (+6.36), 287 (−3.84). UV λ_{max} (MeOH) nm (log ε): 226 (4.31), 282 (4.03). IR ν_{max} (KBr) cm^{-1}: 3400, 1624, 1541, 1510, 1458, 1144, 1069. ^1H and ^{13}C NMR data, see Table 1. Positive-ion FAB-MS *m/z* 633 $[M + Na]^+$. High-resolution FAB-MS *m/z* 633.1792 $[M + Na]^+$ (calcd for $C_{28}H_{34}O_{15}Na$, 633.1795).

Kaempferiaoside D (4)

Amorphous powder, $[\alpha]_D^{23}$ −45.2° (*c* 0.25, MeOH). CD [MeOH, nm (Δε)]: 224 (+7.21), 247 (−6.91), 288 (+1.70). UV λ_{max} (MeOH) nm (log ε): 225 (4.31), 282 (4.01). IR ν_{max} (KBr) cm^{-1}: 3400, 1647, 1541, 1509, 1458, 1144, 1069. ^1H and ^{13}C NMR data, see Table 1. Positive-ion FAB-MS *m/z* 633 $[M + Na]^+$. High-resolution FAB-MS *m/z* 633.1792 $[M + Na]^+$ (calcd for $C_{28}H_{34}O_{15}Na$, 633.1795).

Kaempferiaoside E (5)

White powder, $[\alpha]_D^{25}$ −37.3° (*c* 0.16, MeOH). UV λ_{max} (MeOH) nm (log ε): 231 (3.95), 280 (3.77), 306 (3.71). IR ν_{max} (KBr) cm^{-1}: 3400, 1684, 1593, 1522, 1458, 1281, 1071. ^1H and ^{13}C NMR data, see Table 2. Positive-ion FAB-MS *m/z* 513 $[M + Na]^+$. High-resolution FAB-MS *m/z* 513.1581 $[M + Na]^+$ (calcd for $C_{21}H_{30}O_{13}Na$, 513.1584).

Kaempferiaoside F (6)

White powder, $[\alpha]_D^{23}$ −84.6° (*c* 0.14, MeOH). UV λ_{max} (MeOH) nm (log ε): 223 (4.00), 279 (3.97). IR ν_{max} (KBr) cm^{-1}: 3400, 1628, 1437, 1275, 1183, 1078. ^1H and ^{13}C NMR data, see Table 2. Positive-ion FAB-MS *m/z* 647 $[M + Na]^+$. High-resolution FAB-MS *m/z* 647.1804 $[M + Na]^+$ (calcd for $C_{25}H_{36}O_{18}Na$, 647.1799).

Acid hydrolysis of kaempferiaosides C–F (3–6)

Solutions of **3** (1.1 mg), **4** (1.0 mg), **5** (1.2 mg), and **6** (1.1 mg) in 1 M HCl (1.0 ml) were stirred at 80°C for 1 h. After being cooled, the reaction mixture was neutralized with Amberlite IRA-400 (OH^- form), and the resins were removed by filtration. After removal of the solvent from the filtrate under reduced pressure, the residue was partitioned in an EtOAc–H_2O (1:1, v/v) mixture, and the solvent was removed in vacuo from the EtOAc- and H_2O-soluble fractions. The H_2O-soluble fraction was subjected to HPLC analysis under following conditions: HPLC column, Kaseisorb LC NH_2-60-5, 4.6 mm i.d. × 250 mm (Tokyo Kasei Co., Ltd., Tokyo, Japan); detection, optical rotation [OR-2090 Plus (Jasco, Tokyo, Japan); mobile phase, CH_3CN–H_2O (80:20, v/v); flow rate 1.0 ml min^{-1}]. Identification of D-apiose (i) from **6**, L-rhamnose (ii) from **3** to **5**, and D-glucose (iii) from **3** to **6** present in the H_2O-soluble fraction was carried out by comparison of their retention times (t_R) and optical rotations with those of authentic samples; t_R: (i) 8.4 min (positive optical rotation), (ii) 8.9 min (negative optical rotation) and (iii) 18.7 min (positive optical rotation). Authentic D-apiose was obtained by acid hydrolysis of 1,2,3,5-di-*O*-isopropylidene-α-D-apiose (Funakoshi Co., Ltd. Tokyo, Japan).

Acknowledgments This work was supported by the High-tech Research Center Project for Private Universities: matching fund subsidy from MEXT (The Ministry of Education, Culture, Sports, Science and Technology), 2007-2011, and also supported by a Grant-in Aid for Scientific Research by JSPS (Japan Society for the Promotion of Science).

References

1. Wattanapitayakul SK, Suwatronnakorn M, Chularojmontri L, Herunsalee A, Niumsakul S, Charuchongkolwongse S, Chansuvanich N (2007) *Kaempferia parviflora* ethanolic extract promoted nitric oxide production in human umbilical vein endothelial cells. J Ethopharmacol 110:559–562
2. Wattanapitayakul SK, Chularojmontri L, Herunsalee A, Charuchongkolwongse S, Chansuvanich N (2008) Vasorelaxation and antispasmodic effects of *Kaempferia parviflora* ethanolic extract in isolated rat organ studies. Fitoterapia 79:214–216
3. Tep-areenan P, Sawasdee P, Randall M (2010) Possible mechanisms of vasorelaxation for 5,7-dimethoxyflavone from *Kaempferia parviflora* in the rat aorta. Phytother Res 24:1520–1525
4. Tewtrakul S, Subhadhirasakul S, Kummee S (2008) Anti-allergic activity of compounds from *Kaempferia parviflora*. J Ethnopharmacol 116:191–193
5. Rujjanawate C, Kanjanapothi D, Amornlerdpison D, Pojanagaroon S (2005) Anti-gastric ulcer effect of *Kaempferia parviflora*. J Ethnopharmacol 102:120–122
6. Trisomboon H, Watanabe G, Wetchasit P, Taya K (2007) Effect of daily treatment with Thai herb, *Kaempferia parviflora*, in Hershberger assay using castrated immature rats. J Reprod Dev 53:351–356
7. Trisomboon H, Tohei A, Malaivijitnond S, Watanabe G, Taya K (2008) Oral administration of *Kaempferia parviflora* did not disturb male reproduction in rats. J Reprod Dev 54:375–380
8. Yenjai C, Prasanphen K, Daodee S, Wongpanich V, Kittakoop P (2004) Bioactive flavonoids from *Kaempferia parviflora*. Fitoterapia 75:89–92
9. Tewtrakul S, Subhadhirasakul S (2008) Effects of compounds from *Kaempferia parviflora* on nitric oxide, prostaglandin E_2 and tumor necrosis factor-alpha productions in RAW264.7 macrophage cells. J Ethnopharmacol 120:81–84
10. Tewtrakul S, Subhadhirasakul S, Karalai C, Ponglimanont C (2009) Anti-inflammatory effects of compounds from *Kaempferia parviflora* and *Boesenbergia pandurata*. Food Chem 115:534–538
11. Sea-Wong C, Matsuda H, Tewtrakul S, Tansakul P, Nakamura S, Nomura Y, Yoshikawa M (2011) Suppressive effects of methoxyflavonoids isolated from *Kaempferia parviflora* on inducible nitric oxide synthase (iNOS) expression in RAW264.7 cells. J Ethnopharmacol 136:488–495
12. Azuma T, Kayano S, Matsumura Y, Konishi Y, Tanaka Y, Kikuzaki H (2011) Antimutagenic and α-glucosidase inhibitory effects of constituents from *Kaempferia parviflora*. Food Chem 125:471–475
13. Nakao K, Murata K, Deguchi T, Itoh K, Fujita T, Higashino M, Yoshioka Y, Matsumura S, Tanaka R, Shinada T, Ohfune Y, Matsuda H (2011) Xanthine oxidase inhibitory activities and crystal structures of methoxyflavones from *Kaempferia parviflora* rhizome. Biol Pharm Bull 34:1143–1146
14. Wanich S, Yenjai C (2009) Amino and nitro derivatives of 5,7-dimethoxyflavone from *Kaempferia parviflora* and cytotoxicity against KB cell line. Arch Pharm Res 32:1185–1189
15. Yenjai C, Wanich S (2010) Cytotoxicity against KB and NCI-H187 cell lines of modified flavonoids from *Kaempferia parviflora*. Bioorg Med Chem Lett 20:2821–2823
16. Patanasethanont D, Nagai J, Yumoto R, Murakami T, Sutthanut K, Sripanidkulchai B, Yenjai C, Takano M (2007) Effects of *Kaempferia parviflora* extracts and their flavone constituents on P-glycoprotein function. J Pharm Sci 96:223–233
17. Patanasethanont D, Nagai J, Matsuura C, Fukui K, Sutthanut K, Sripanidkulchai B, Yumoto R, Takano M (2007) Modulation of function of multidrug resistance associated-proteins by *Kaempferia parviflora* extracts and their components. Eur J Pharmacol 566:67–74
18. Akase T, Shimada T, Terabayashi S, Ikeya Y, Sanada H, Aburada M (2011) Antiobesity effects of *Kaempferia parviflora* in spontaneously obese type II diabetic mice. J Nat Med 65:73–80
19. Chaipech S, Morikawa T, Ninomiya K, Yoshikawa M, Pongpiriyadacha Y, Hayakawa T, Muraoka O (2011) Structures of two new phenolic glycosides, kaempferiaosides A and B, and hepatoprotective constituents from the rhizomes of *Kaempferia parviflora*. Chem Pharm Bull 60(1): online (http://denshi.pharm.or.jp/home/pubpharm/pubview.asp?p=c110371) (http://denshi.pharm.or.jp/home/pubpharm/pubpharm.asp?JID=CPB)
20. Clark-Lewis JW (1968) Flavan derivatives XXI. Nuclear magnetic resonance spectra, configuration, and conformation of flavan derivatives. Aust J Chem 21:2059–2075
21. Zanarotti A (1982) Synthesis of a flav-3-en-3-ol via cinnamylphenol. Tetrahedron Lett 23:3963–3964
22. Stafford HA (1983) Enzymic regulation of procyanidin biosynthesis; lack of a flav-3-en-3-ol intermediate. Phytochemistry 22:2643–2646
23. Morikawa T, Li X, Nishida E, Nakamura S, Ninomiya K, Matsuda H, Hamao M, Muraoka O, Hayakawa T, Yoshikawa M (2011) Medicinal flowers. XXXII. Structures of oleanane-type

triterpene saponins, perennisosides VIII, IX, X, XI, and XII, from the flowers of Bellis perennis. Chem Pharm Bull 59:889–895
24. Coetzee J, Malan E, Ferreira D (2000) Synthesis and reactions of flav-3-en-3-ols. Tetrahedron 56:1819–1824
25. Jiu-zhi Y, De-qiang D, Ying-jie C, Wei L, Koike K, Nikaido T, Xin-sheng X (2004) Phenolic glycosides from rhizome of *Smilax glabra*. Chin Trad Herb Drugs 35:967–969

Analytical Biochemistry 431 (2012) 120–126

Contents lists available at SciVerse ScienceDirect

Analytical Biochemistry

journal homepage: www.elsevier.com/locate/yabio

Specific detection of *N*-glycolylneuraminic acid and Galα1–3Gal epitopes of therapeutic antibodies by partial-filling capillary electrophoresis

Yuki Yagi [a,*], Kazuaki Kakehi [b], Takao Hayakawa [b], Yukihito Ohyama [a], Shigeo Suzuki [b]

[a] *Kyowa Hakko Kirin Co., Ltd., Takasaki, Gunma 370-0013, Japan*
[b] *Faculty of Pharmaceutical Sciences, Kinki University, Higashi-Osaka, Japan*

ARTICLE INFO

Article history:
Received 4 June 2012
Received in revised form 1 September 2012
Accepted 4 September 2012
Available online 11 September 2012

Keywords:
N-glycolylneuraminic acid
Galα1–3Gal
Myeloma cells
Immunoglobulin
Oligosaccharide
Partial-filling affinity electrophoresis

ABSTRACT

The oligosaccharide structure is very important in biopharmaceuticals because of its effects on protein function, including efficacy and half-life. *N*-Glycolylneuraminic acid (Neu5Gc) and Galα1–3Gal (α-Gal) residues are known to show immunogenicity in humans. It is now understood that murine cell lines, such as NS0 or SP2, which are typically used for biopharmaceutical manufacture, produce proteins containing Neu5Gc and α-Gal residues. The expression of these specific residues is affected by the cell line and culture conditions. Therefore, monitoring and controlling the levels of these epitopes are important for the quality control of biopharmaceuticals. To detect the two epitopes on a therapeutic antibody produced by NS0 cells, we applied partial-filling capillary electrophoresis using anti-Neu5Gc antibody and α-galactosidase. In the anti-Neu5Gc antibody filling method, one minor glycan peak with Neu5Gc residues at the nonreducing end disappeared specifically from the electropherogram. In the α-galactosidase filling method, some minor peaks with α1,3-linked Gal residues disappeared. However, in a therapeutic antibody from Chinese hamster ovary cells, no peaks disappeared with the two methods. These results show this method can be used to specifically detect and quantify the two epitopes on biopharmaceuticals with high sensitivity.

More than 20 pharmaceutical antibodies have been approved for treatment of cancers, autoimmune disorders, and inflammation [1,2]. Antibodies are becoming important agents for medical treatment because of their high specificity and low toxicity. Antibody molecules contain glycosylation sites that bear various oligosaccharides depending on the cell lines used for antibody production [3,4].

Some therapeutic antibodies produced by mouse myeloma cells, such as SP2 or NS0 cells, are known to generate *N*-glycolylneuraminic acid (Neu5Gc)[1] and Galα1–3Gal (α-Gal), which show immunogenicity in humans [5–11]. In addition, some reported Chinese hamster ovary (CHO) cells can produce α-Gal [12,13]. Neu5Gc is known to induce immune responses in humans. Anti-Neu5Gc antibodies have been detected in 85% of the human population, sometimes at high levels [14,15,10]. In addition, high Neu5Gc levels on proteins are associated with rapid clearance profiles in vivo [16]. α-Gal is strongly immunogenic in humans and over 1% of serum IgG is directed against the residue [17]. The presence of α-Gal attributed to a murine myeloma cell line mainly causes adverse clinical events associated with an induced IgE-mediated anaphylaxis response in patients treated with the commercial antibody cetuximab [18,19]. Some reports suggest that these glycan epitope expressions are affected by cell lines and culture conditions [6,7,20–22]. Controlling the levels of this antigenic epitope during development of biotherapeutics could have a positive impact on the safety and clearance of the drug.

Several analytical techniques have been used for detection and quantification of the glycan epitopes. These include high-pH anion-exchange chromatography with pulsed amperometric detection [23], HPLC with fluorescence labeling [24], liquid chromatography coupled with MS [13,25–27], enzyme-linked immunosorbent assay [28,29], and detection by lectins [30–33]. However, there are few cases in which capillary electrophoresis has been used for detection of the epitopes. Capillary electrophoresis with laser-induced fluorescence detection (CE-LIF) provides rapid, high-resolution, and highly sensitive analysis of fluorescence-labeled oligosaccharides. In particular, 8-aminopyrene-1,3,6-trisulfonate (APTS) has been widely used for analysis of oligosaccharides derived from antibody pharmaceuticals [34–39]. Three sulfonate groups of APTS induce rapid movement of labeled oligosaccharides, and the oligosaccharides in antibodies undergo complete resolution by CE-LIF. In addition, the partial-filling technique has been used to ascertain the affinity characteristics between receptors and ligands [40–53]. In this technique, the capillary is partly filled with the affinity ligand dissolved in running buffer before injection of the sample. The pH of the running buffer is selected to sustain the affinity of ligand proteins, and the sample must be moved quickly across the "plug" of ligand in an electric

* Corresponding author. Fax: +81 27 352 4977.
E-mail address: yuuki.yagi@kyowa-kirin.co.jp (Y. Yagi).

[1] *Abbreviations used:* Neu5Gc, *N*-glycolylneuraminic acid; α-Gal, Galα1–3Gal; CHO, Chinese hamster ovary; CE-LIF, capillary electrophoresis with laser-induced fluorescence detection; APTS, 8-aminopyrene-1,3,6-trisulfonic acid; GSL I-B_4, *Griffonia simplicifolia* I-B_4; PFACE, partial-filling affinity capillary electrophoresis.

0003-2697/$ - see front matter © 2012 Elsevier Inc. All rights reserved.
http://dx.doi.org/10.1016/j.ab.2012.09.006

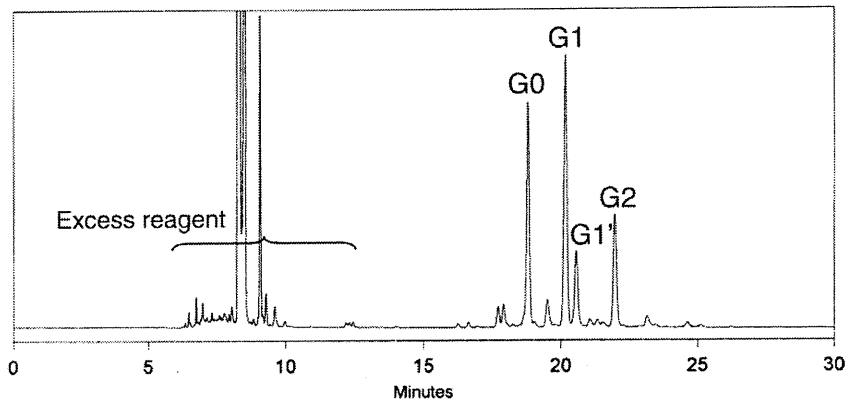

Fig.1. Typical electropherogram of APTS-labeled oligosaccharides derived from palivizumab. Analytical conditions: capillary, DB-1 (total length, 40 cm; effective length, 30 cm; 50 μm i.d.); running buffer, 100 mM Tris–acetic acid buffer (pH 7.0) with 0.05% hydroxypropyl cellulose; applied voltage, −15 kV at 25 °C; sample injection, 3.4 kPa, for 15 s.

field. When a voltage is applied, the sample migrates through the plug of affinity ligand. Sample components with affinity to the ligand phase are trapped, and those that do not have affinity reach the detector without retardation. This technique does not require chemical immobilization of the ligand molecules.

In an earlier study, we applied the partial-filling affinity capillary electrophoresis (PFACE) method with lectins and enzymes for the analysis of APTS-labeled oligosaccharides obtained from a therapeutic antibody [54]. However, there are no lectins and enzymes that specifically interact or react with the Neu5Gc residue. Therefore, in this study, we applied the anti-Neu5Gc antibody to the PFACE method. In addition, because of the unknown specificity of *Griffonia simplicifolia* I-B_4 (GSL I-B_4), which is currently used for detection of α-Gal in histochemistry [30–33], we chose α-galactosidase for detection of α-Gal residues.

Materials and methods

Materials

The following materials were used in this study: palivizumab (Medimmune, Gaithersburg, MD, USA), rituximab (Genentech, San Francisco, CA, USA), *N*-glycosidase F (Roche Diagnostics, Mannheim, Germany), APTS (Beckman–Coulter, Fullerton, CA, USA), acetic acid and tetrahydrofuran (Wako Pure Chemical Industries, Tokyo, Japan), sodium cyanoborohydride (Sigma–Aldrich, St. Louis, MO, USA), hydroxypropyl cellulose (3–6 mPa/s; Tokyo Chemical Industry Co., Ltd, Tokyo, Japan), DB-1 capillary (J&W Scientific, Folsom, CA, USA), NAP-5 columns (GE Healthcare Life Sciences, Piscataway, NJ, USA), 2-mercaptoethanol (Nacalai Tesque, Tokyo, Japan), anti-Neu5Gc polyclonal antibody (Sialix, Vista, CA, USA), α2-3,6,8,9-neuraminidase (*Arthrobacter ureafaciens*) (Nacalai Tesque), lectin from GSL I-B_4 (Vector Laboratories, Burlingame, CA, USA), α1–3,4,6-galactosidase (green coffee bean) (ProZyme, Hayward, CA, USA), and β1–4-galactosidase (Calbiochem, Hayward, CA, USA).

Release of N-linked oligosaccharides from therapeutic antibodies

Antibody (50 μl, 500 μg) was mixed with 2-mercaptethanol (1 μl) and 1 U/μl of *N*-glycosidase F (15 μl). The mixture was incubated at 37 °C overnight. After digestion, 154 μl of ice-cold ethanol was added, and the mixture was centrifuged (10,000*g* for 15 min at 4 °C) to remove proteins. The supernatant was dried using a centrifugal vacuum evaporator.

Fluorescence derivatization of oligosaccharides with APTS

Oligosaccharides were labeled according to an established method [54]. Briefly, the dry sample was dissolved in 3 μl of 0.2 M APTS in 15% (v/v) acetic acid and then mixed with 3 μl

Table 1
Structures of the major oligosaccharides derived from palivizumab and their relative corrected peak areas.

Name	Structure	Relative corrected peak area (%)
G0	GlcNAcβ1-2Manα1\6 / GlcNAcβ1-2Manα1/3 Fucα1\6 Manβ1-4GlcNAcβ1-4GlcNAc	26.9
G1	Galβ1-4GlcNAcβ1-2Manα1\6 / GlcNAcβ1-2Manα1/3 Fucα1\6 Manβ1-4GlcNAcβ1-4GlcNAc	32.4
G1'	GlcNAcβ1-2Manα1\6 / Galβ1-4GlcNAcβ1-2Manα1/3 Fucα1\6 Manβ1-4GlcNAcβ1-4GlcNAc	10.0
G2	Galβ1-4GlcNAcβ1-2Manα1\6 / Galβ1-4GlcNAcβ1-2Manα1/3 Fucα1\6 Manβ1-4GlcNAcβ1-4GlcNAc	13.2

The relative corrected peak area (%) was calculated as follows: corrected peak area = (measured peak area)/(migration time), relative corrected peak area (%) = [(corrected peak area)/(total corrected peak area)] × 100.

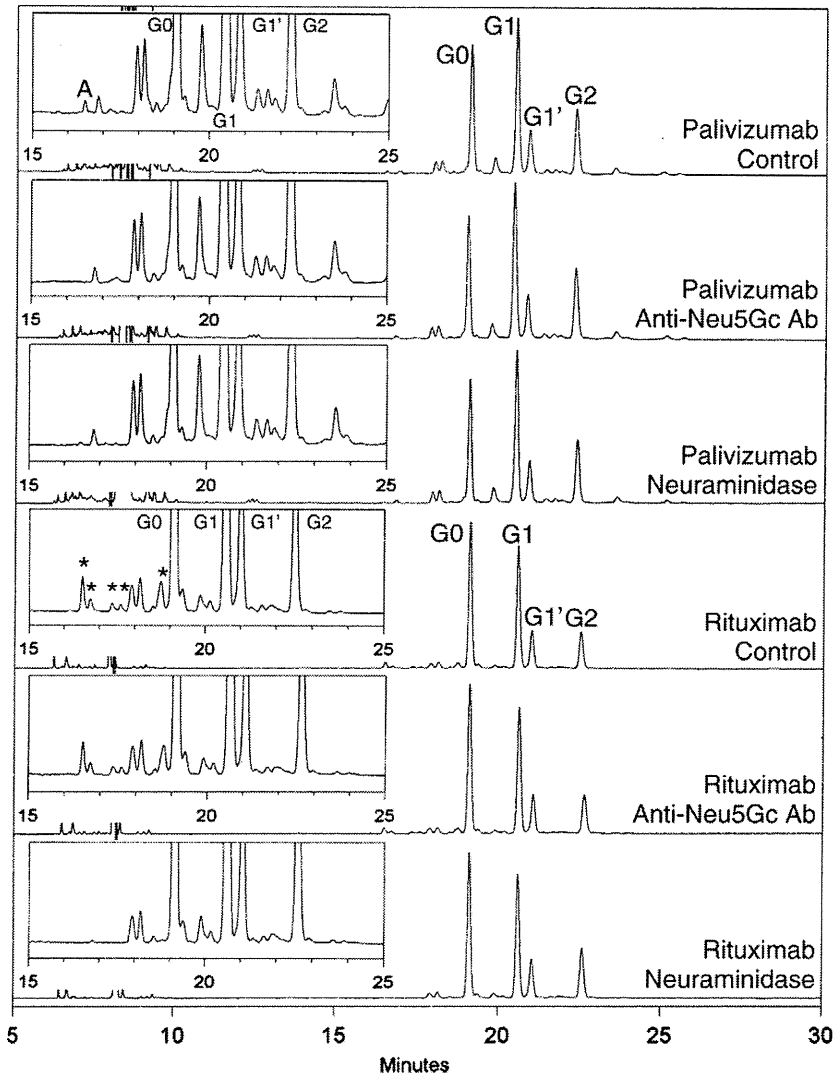

Fig.2. Partial-filling affinity electrophoresis with anti-Neu5Gc antibody (Ab) and partial-filling enzymatic digestion with α2–3,6,8,9-neuraminidase (5 U/ml) of APTS-labeled oligosaccharides from palivizumab and rituximab. Capillary electrophoresis conditions: lectin injection, 3.4 kPa, for 60 s. Other conditions were identical to those for Fig. 1.

of a 1 M sodium cyanoborohydride solution in tetrahydrofuran. The mixture was heated at 55 °C for 90 min and then mixed with 94 μl of water before being applied to a NAP-5 column previously equilibrated with 10 ml of water. APTS–oligosaccharides were recovered by elution with 600 μl of water. The eluate from the column was dried with a centrifugal vacuum evaporator, and the residue was dissolved in 1 ml of water for capillary electrophoresis.

Capillary electrophoresis of APTS-labeled oligosaccharides

The capillary electrophoresis system used in this study was a PA-800 system (Beckman–Coulter) with an argon laser-induced fluorescence detector (excitation wavelength 488 nm; emission wavelength 520 nm). A DB-1 capillary (50 μm i.d.; effective length, 30 cm; total length, 40 cm) was used with 100 mM Tris–acetic acid buffer (pH 7.0) with 0.05% hydroxypropyl cellulose as the running buffer. Sample solutions were introduced to the capillary under pressure (3.4 kPa). A voltage of −15 kV was applied at 25 °C for 30 min. Before each run, the capillary was rinsed with 0.1 M NaOH at 103 kPa for 10 min, water at 103 kPa for 5 min, and the running buffer at 103 kPa for 7 min.

Partial-filling capillary electrophoresis

Antibody, lectin, and enzymes were diluted with the running buffer. Before a sample solution was introduced, the antibody (or lectin, enzyme) solution was introduced into the capillary under pressure (3.4 kPa; 60 s). The samples were separated under the same conditions as described above.

Results and discussion

CE-LIF analysis of N-linked glycan structure from palivizumab

Palivizumab, which is a recombinant antibody against respiratory syncytial virus, has an N-linked oligosaccharide at each Fc region. A typical electropherogram for the analysis of APTS-labeled oligosaccharides from palivizumab is shown in Fig. 1. Peaks appeared between 6 and 13 min for the reagents, while peaks for the APTS-labeled oligosaccharides were observed between 16 and 26 min. The main oligosaccharides of palivizumab and their corrected peak areas are shown in Table 1. Palivizumab contains the following four major oligosaccharides: G0, an agalactosylated oligosaccharide; G1 and G1′, monogalactosylated oligosaccharides

II NeuAcα2-6{Galβ1-4GlcNAcβ1-2Manα1\6, Galβ1-4GlcNAcβ1-2Manα1/3}Manβ1-4GlcNAcβ1-4GlcNAc, Fucα1\6

III Galα1-3 NeuAcα2-6{Galβ1-4GlcNAcβ1-2Manα1\6, Galβ1-4GlcNAcβ1-2Manα1/3}Manβ1-4GlcNAcβ1-4GlcNAc, Fucα1\6

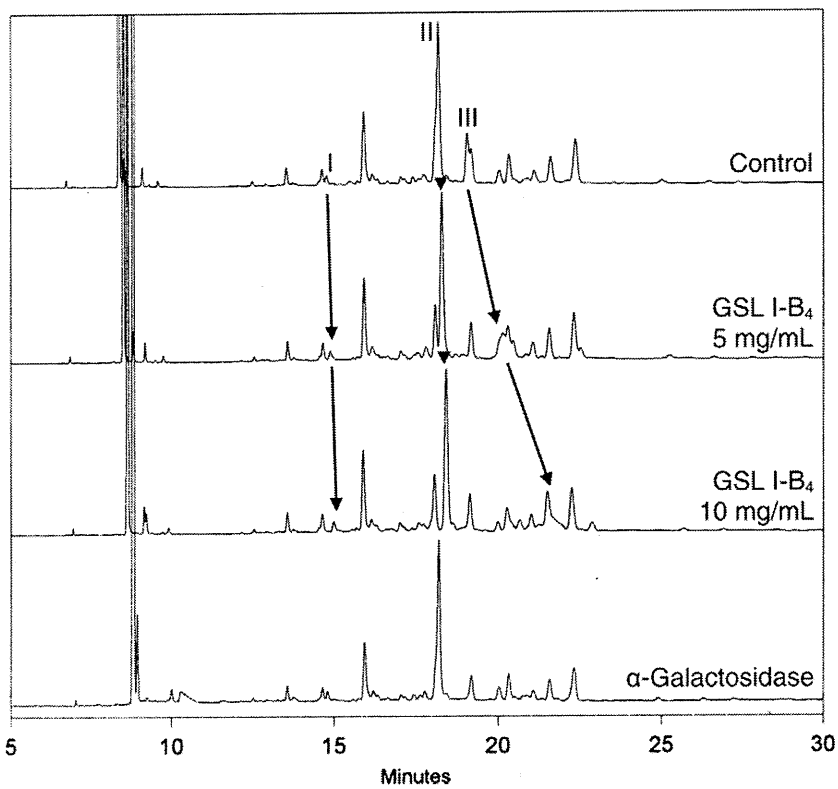

Fig.3. Partial-filling affinity electrophoresis with GSL I-B_4 and partial-filling enzymatic digestion with α1–3,4,6-galactosidase (75 U/ml) of APTS-labeled oligosaccharides from porcine thyroglobulin. Capillary electrophoresis conditions were identical to those for Fig. 2.

with two positional isomers; and G2, a fully galactosylated oligosaccharide. In addition, palivizumab should have some Neu5Gc and α-Gal at the nonreducing terminals of its N-linked glycan because the antibody is produced from NS0 cells [5–8].

We have previously shown that CE-LIF is suitable for the determination and characterization of APTS oligosaccharides derived from an antibody, because it has high reproducibility [54]. The results showed high reproducibility, with relative SDs of less than 0.6% (SD $\leqslant$ 0.1%) for the relative corrected peak areas and less than 0.1% for migration times with three independent preparations from rituximab, which is a recombinant antibody used for the treatment of non-Hodgkin lymphoma.

Specific detection of Neu5Gc residues using PFACE with anti-Neu5Gc antibody

Because there are no lectins or enzymes that interact with or hydrolyze Neu5Gc residues specifically, we used anti-Neu5Gc antibody, which is a chicken polyclonal IgY [55]. This antibody is highly specific to Neu5Gc residues found in oligosaccharides and glycoproteins. After introduction of 2.6 μM anti-Neu5Gc antibody solution to the capillary, the APTS-labeled oligosaccharides from palivizumab were injected and separated. The resultant electropherogram (Fig. 2) showed that anti-Neu5Gc antibody caused the disappearance of a minor peak at around 16.5 min (peak A). The corrected peak area ratio of peak A to total saccharide peaks was 0.4%. Peak A disappeared after partial-filling enzymatic digestion [54] with α2–3,6,8,9-neuraminidase. These results show that peak A is a glycan with Neu5Gc residues at the nonreducing ends. By contrast, though some glycan peaks, marked by asterisks, from rituximab produced from CHO cells disappeared after digestion with α2–3,6,8,9-neuraminidase, no peaks disappeared with preinjection of anti-Neu5Gc antibody (Fig. 2). This result shows that rituximab has no Neu5Gc residues and is consistent with an earlier detailed study of the glycan profile of rituximab [56].

These studies confirmed that PFACE with anti-Neu5Gc antibody can detect Neu5Gc residues on oligosaccharides from biopharmaceuticals with high specificity and sensitivity. In addition, the combination of PFACE with various kinds of lectins and exoglycosidases will provide additional detailed information about glycan branches [54].

Specific detection of α-Gal residues using partial-filling enzymatic digestion in capillary electrophoresis with α-galactosidase

GSL I-B_4 is specific for terminal α-Gal residues and is used to detect the α-Gal epitope in xenotransplantation research [30,33]. However, when evaluating the specificity of this lectin to porcine thyroglobulin, we surprisingly observed unfamiliar specificity of this lectin. Partial-filling GSL I-B_4 capillary electrophoresis of saccharides from porcine thyroglobulin showed weak interaction with a monosialylated biantennary complex-type glycan (peak II) which

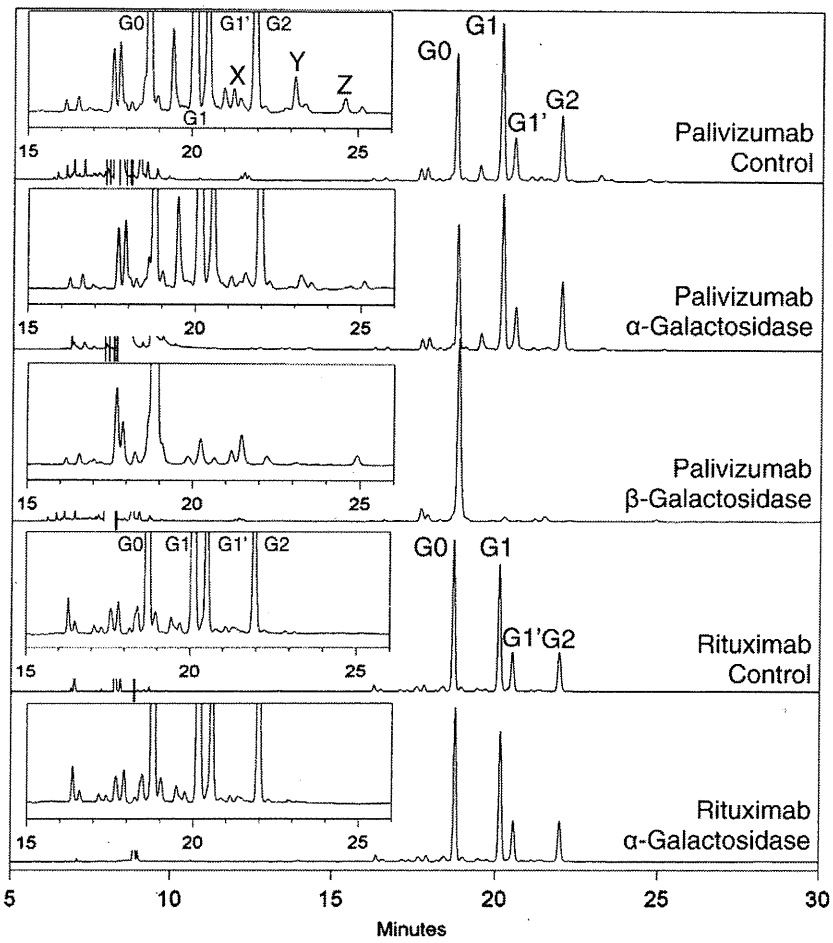

Fig.4. Partial-filling enzymatic digestion of APTS-labeled oligosaccharides from palivizumab and rituximab using α1–3,4,6-galactosidase (75 U/ml). Capillary electrophoresis conditions were identical to those for Fig. 2.

has no α-Gal residues at the nonreducing end. We also observed the weak interaction with peak I, but its oligosaccharide structure is unknown (Fig. 3) [57]. These results show the lectin unsuitable for determining α-Gal residues. Therefore, we chose α1–3,4,6-galactosidase (α-galactosidase) for detection of α-Gal residues. It also hydrolyzes α1,4-linked Gal and α1,6-linked Gal residues. However, α1,4-linked Gal and α1,6-linked Gal residues are uncommon in mammal glycoproteins [58]. Therefore, the α-Gal residues digested by α-galactosidase on the oligosaccharides from pharmaceutical antibodies must be α1,3-linked Gal residues.

After introduction of 75 U/ml α-galactosidase to the capillary, the APTS-labeled oligosaccharides from palivizumab were injected and separated. A minor peak (Z) disappeared, and two peaks (X and Y) decreased in size (Fig. 4). Because the concentration of the enzyme was enough to hydrolyze α1,3-linked Gal residues in thyroglobulin glycan, peaks X and Y were thought to be a mixture of two or more kinds of glycans with and without α-Gal residues. The corrected peak area ratios of peaks X, Y, and Z were 0.6%, 0.8%, and 0.6%, respectively. The peak ratios of X and Y do not show the whole ratio, but the proportion decreased by the digestion. We used MS to confirm that palivizumab has a series of biantennary complex-type glycans with additional one and two hexose residues (data not shown). Moreover, in the partial-filling enzymatic digestion with β1–4-galactosidase, peak Y disappeared and peak Z did not (Fig. 4). This result shows that peak Y has β1,4-linked Gal residues on its nonreducing end and peak Z does not. The neutral APTS–glycans have the same net charges, and the separation is based on the differences in their apparent hydrodynamic sizes. The glycans migrate in order of increasing size (G0 < G1 < G2 < G2 + hexose, etc.), and it is presumed that peak Y is for G2 with an additional α1,3-linked Gal residue and peak Z is for G2 with two α1,3-linked Gal residues. Although peak X was thought to contain a glycan with α-Gal residues, its structure was not clear. We also confirmed that α-galactosidase showed specific hydrolysis of α-Gal residues on porcine thyroglobulin oligosaccharides (Fig. 3). Peak III, which contains α-Gal residues, disappeared after digestion in CE with α-galactosidase, while peaks I and II did not disappear. Rituximab contains no α-Gal residues because there was no peak that disappeared with α-galactosidase digestion (Fig. 4).

These studies show that α-Gal residues could be detected specifically with partial-filling enzymatic digestion. Although the specific levels of α-Gal required to induce anaphylaxis reactions are not well known and are likely to be product dependent [13], control of the α-Gal content in antibody pharmaceuticals is important to prevent anaphylaxis reactions. Therefore, the high sensitivity of this method makes it suitable for monitoring of α-Gal residues during the development of biopharmaceuticals.

Concluding remarks

HPLC and MS with fluorescence labeling are usually used to detect and quantify Neu5Gc residues because there are no specific glycosidases and lectins [8,25,59]. By contrast, HPLC or MS with α-galactosidase digestion is used for detection of α-Gal residues [5,6,13,60]. Consequently, Neu5Gc and α-Gal cannot be detected simultaneously and conveniently. We used partial-filling CE for

detection of the two glycan epitopes in pharmaceutical recombinant antibodies. This method makes it possible to detect and quantify the two antigens on the biopharmaceuticals in the same analytical sequence.

In this study, 40 μl of a 1-ml preparation of APTS-labeled glycan from palivizumab (500 μg) was used in CE analysis. Therefore, theoretically, about 20 μg of antibody sample can detect about 0.4% of glycan epitopes.

It is important to investigate and improve cell culture conditions for the manufacture of high-quality biopharmaceuticals in high yield. Neu5Gc and α-Gal epitopes are the most important modifications and should be carefully monitored and controlled in manufacturing processes. The simplicity and high sensitivity of this method will be valuable for detection of glycan epitopes during development of the biopharmaceutical manufacturing process.

Since biopharmaceuticals are mainly produced by CHO cells or mouse myeloma cells, it is not necessary to detect and quantify any antigens other than Neu5Gc and α-Gal. However, in recent years, production methods of biopharmaceuticals using transgenic plants [61–64] and insects [65–67] have been under development. Plants and insects are known to generate β1,2-linked xylose and/or α1,3-linked fucose on their N-linked glycans, and these epitopes cause immune responses in humans [63,68–70]. Our analytical method would be applicable for detecting these novel antigens using affinity molecules, such as antibodies, lectins, or exoglycosidases, to the antigens.

Acknowledgment

This work was supported by a Grant-in-Aid for Scientific Research (C) from the Japan Society for the Promotion of Science, 2011–2013.

References

[1] L.M. Weiner, R. Surana, S. Wang, Monoclonal antibodies: versatile platforms for cancer immunotherapy, Nat. Rev. Immunol. 10 (2010) 317–327.
[2] A.C. Chan, P.J. Carter, Therapeutic antibodies for autoimmunity and inflammation, Nat. Rev. Immunol. 10 (2010) 301–316.
[3] Y.G. Kim, G.C. Gil, K.S. Jang, S. Lee, H.I. Kim, J.S. Kim, J. Chung, C.G. Park, D.J. Harvey, B.G. Kim, Qualitative and quantitative comparison of N-glycans between pig endothelial and islet cells by high-performance liquid chromatography and mass spectrometry-based strategy, J. Mass Spectrom. 44 (2009) 1087–1104.
[4] J.A. Serrato, V. Hernández, S. Estrada-Mondaca, L.A. Palomares, O.T. Ramírez, Differences in the glycosylation profile of a monoclonal antibody produced by hybridomas cultured in serum-supplemented, serum-free or chemically defined media, Biotechnol. Appl. Biochem. 47 (2007) 113–124.
[5] D.M. Sheeley, B.M. Merrill, L.C. Taylor, Characterization of monoclonal antibody glycosylation: comparison of expression systems and identification of terminal alpha-linked galactose, Anal. Biochem. 247 (1997) 102–110.
[6] K.N. Baker, M.H. Rendall, A.E. Hills, M. Hoare, R.B. Freedman, D.C. James, Metabolic control of recombinant protein N-glycan processing in NS0 and CHO cells, Biotechnol. Bioeng. 73 (2001) 188–202.
[7] E.M. Yoo, K.R. Chintalacharuvu, M.L. Penichet, S.L. Morrison, Myeloma expression systems, J. Immunol. Methods 261 (2002) 1–20.
[8] A. Beck, E. Wagner-Rousset, M.C. Bussat, M. Lokteff, C. Klinguer-Hamour, J.F. Haeuw, L. Goetsch, T. Wurch, A. Van Dorsselaer, N. Corvaïa, Trends in glycosylation, glycoanalysis and glycoengineering of therapeutic antibodies and Fc-fusion proteins, Curr. Pharm. Biotechnol. 9 (2008) 482–501.
[9] A. Noguchi, C.J. Mukuria, E. Suzuki, M. Naiki, Immunogenicity of N-glycolylneuraminic acid-containing carbohydrate chains of recombinant human erythropoietin expressed in Chinese hamster ovary cells, J. Biochem. 117 (1995) 59–62.
[10] V. Padler-Karavani, H. Yu, H. Cao, H. Chokhawala, F. Karp, N. Varki, X. Chen, A. Varki, Diversity in specificity, abundance, and composition of anti-Neu5Gc antibodies in normal humans: potential implications for disease, Glycobiology 18 (2008) 818–830.
[11] B.A. Macher, U. Galili, The Galalpha1, 3Galbeta1, 4GlcNAc-R (alpha-Gal) epitope: a carbohydrate of unique evolution and clinical relevance, Biochim. Biophys. Acta 1780 (2008) 75–88.
[12] D.A. Ashford, C.D. Alafi, V.M. Gamble, D.J. Mackay, T.W. Rademacher, P.J. Williams, R.A. Dwek, A.N. Barclay, S.J. Davis, C. Somoza, Site-specific glycosylation of recombinant rat and human soluble CD4 variants expressed in Chinese hamster ovary cells, J. Biol. Chem. 268 (1993) 3260–3267.
[13] C.J. Bosques, B.E. Collins, J.W. Meador, H. Sarvaiya, J.L. Murphy, G. Dellorusso, D.A. Bulik, I.H. Hsu, N. Washburn, S.F. Sipsey, J. Myette, R. Raman, Z. Shriver, R. Sasisekharan, G. Venkataraman, Chinese hamster ovary cells can produce galactose-α-1,3-galactose antigens on proteins, Nat. Biotechnol. 28 (2010) 1153–1156.
[14] A. Zhu, R. Hurst, Anti-N-glycolylneuraminic acid antibodies identified in healthy human serum, Xenotransplantation 9 (2002) 376–381.
[15] P. Tangvoranuntakul, P. Gagneux, S. Diaz, M. Bardor, N. Varki, A. Varki, E. Muchmore, Human uptake and incorporation of an immunogenic nonhuman dietary sialic acid, Proc. Natl. Acad. Sci. USA 100 (2003) 12045–12050.
[16] A.R. Flesher, J. Marzowski, W.C. Wang, H.V. Raff, Fluorophore-labeled carbohydrate analysis of immunoglobulin fusion proteins: correlation of oligosaccharide content with in vivo clearance profile, Biotechnol. Bioeng. 46 (1995) 399–407.
[17] R.M. Hamadeh, G.A. Jarvis, U. Galili, R.E. Mandrell, P. Zhou, J.M. Griffiss, Human natural anti-Gal IgG regulates alternative complement pathway activation on bacterial surfaces, J. Clin. Invest. 89 (1992) 1223–1235.
[18] C.H. Chung, B. Mirakhur, E. Chan, Q.T. Le, J. Berlin, M. Morse, B.A. Murphy, S.M. Satinover, J. Hosen, D. Mauro, R.J. Slebos, Q. Zhou, D. Gold, T. Hatley, D.J. Hicklin, T.A. Platts-Mills, Cetuximab-induced anaphylaxis and IgE specific for galactose-alpha-1,3-galactose, N. Engl. J. Med. 358 (2008) 1109–1117.
[19] S.P. Commins, T.A. Platts-Mills, Allergenicity of carbohydrates and their role in anaphylactic events, Curr. Allergy Asthma Rep. 10 (2010) 29–33.
[20] N. Jenkins, R.B. Parekh, D.C. James, Getting glycosylation right: implications for the biotechnology industry, Nat. Biotechnol. 14 (1996) 975–981.
[21] M. Butler, Animal cell cultures: recent achievements and perspectives in the production of biopharmaceuticals, Appl. Microbiol. Biotechnol. 68 (2005) 283–291.
[22] M.C. Borys, N.G. Dalal, N.R. Abu-Absi, S.F. Khattak, Y. Jing, Z. Xing, Z.J. Li, Effects of culture conditions on N-glycolylneuraminic acid (Neu5Gc) content of a recombinant fusion protein produced in CHO cells, Biotechnol. Bioeng. 105 (2010) 1048–1057.
[23] J.S. Rohrer, J. Thayer, M. Weitzhandler, N. Avdalovic, Analysis of the N-acetylneuraminic acid and N-glycolylneuraminic acid contents of glycoproteins by high-pH anion-exchange chromatography with pulsed amperometric detection, Glycobiology 8 (1998) 35–43.
[24] K.R. Anumula, Rapid quantitative determination of sialic acids in glycoproteins by high-performance liquid chromatography with a sensitive fluorescence detection, Anal. Biochem. 230 (1995) 24–30.
[25] N. Morimoto, M. Nakano, M. Kinoshita, A. Kawabata, M. Morita, Y. Oda, R. Kuroda, K. Kakehi, Specific distribution of sialic acids in animal tissues as examined by LC-ESI-MS after derivatization with 1,2-diamino-4,5-methylenedioxybenzene, Anal. Chem. 73 (2001) 5422–5428.
[26] C.J. Shaw, H. Chao, B. Xiao, Determination of sialic acids by liquid chromatography–mass spectrometry, J. Chromatogr. A 913 (2001) 365–370.
[27] Y.G. Kim, G.C. Gil, D.J. Harvey, B.G. Kim, Structural analysis of alpha-Gal and new non-Gal carbohydrate epitopes from specific pathogen-free miniature pig kidney, Proteomics 8 (2008) 2596–2610.
[28] D. Ghaderi, R.E. Taylor, V. Padler-Karavani, S. Diaz, A. Varki, Implications of the presence of N-glycolylneuraminic acid in recombinant therapeutic glycoproteins, Nat. Biotechnol. 28 (2010) 863–867.
[29] M. Morisset, C. Richard, C. Astier, S. Jacquenet, A. Croizier, E. Beaudouin, V. Cordebar, F. Morel-Codreanu, N. Petit, D.A. Moneret-Vautrin, G. Kanny, Anaphylaxis to pork kidney is related to IgE antibodies specific for galactose-alpha-1,3-galactose, Allergy 67 (2012) 699–704.
[30] R.H. Chen, A. Kadner, J. Tracy, D. Santerre, D.H. Adams, Differential detection of alpha-gal and human CD59 molecules on pig-to-primate cardiac xenotransplantation: a marker of delayed xenograft rejection, Transplant. Proc. 33 (2001) 732–735.
[31] H.C. Winter, K. Mostafapour, I.J. Goldstein, The mushroom Marasmius oreades lectin is a blood group type B agglutinin that recognizes the Galalpha 1,3Gal and Galalpha 1,3Galbeta 1,4GlcNAc porcine xenotransplantation epitopes with high affinity, J. Biol. Chem. 277 (2002) 14996–15001.
[32] E.C. Hallberg, V. Strokan, T.D. Cairns, M.E. Breimer, B.E. Samuelsson, Chemical and lectin-gold electron microscopical studies of the expression of the Galalpha1-determinant in the pig aorta, Xenotransplantation 5 (1998) 246–256.
[33] H. Chi, M. Sato, M. Yoshida, K. Miyoshi, Expression analysis of an α-1,3-galactosyltransferase, an enzyme that creates xenotransplantation-related α-Gal epitope, in pig preimplantation embryos, Anim. Sci. J. 83 (2012) 88–93.
[34] S. Ma, W. Nashabeh, Carbohydrate analysis of a chimeric recombinant monoclonal antibody by capillary electrophoresis with laser-induced fluorescence detection, Anal. Chem. 71 (1999) 5185–5192.
[35] A. Guttman, F.T. Chen, R.A. Evangelista, Separation of 1-aminopyrene-3,6,8-trisulfonate-labeled asparagine-linked fetuin glycans by capillary gel electrophoresis, Electrophoresis 17 (1996) 412–417.
[36] T.S. Raju, J.B. Briggs, S.M. Borge, A.J. Jones, Species-specific variation in glycosylation of IgG: evidence for the species-specific sialylation and branch-specific galactosylation and importance for engineering recombinant glycoprotein therapeutics, Glycobiology 10 (2000) 477–486.
[37] J.S. Patrick, B.P. Rener, G.S. Clanton, A.L. Lagu, Analysis of neutral N-linked oligosaccharides from antibodies using free-solution capillary electrophoresis in bare fused-silica capillaries, Methods Mol. Biol. 276 (2004) 137–151.
[38] L.A. Gennaro, O. Salas-Solano, S. Ma, Capillary electrophoresis–mass spectrometry as a characterization tool for therapeutic proteins, Anal. Biochem. 355 (2006) 249–258.

[39] L.A. Gennaro, O. Salas-Solano, On-line CE-LIF-MS technology for the direct characterization of N-linked glycans from therapeutic antibodies, Anal. Chem. 80 (2008) 3838–3845.
[40] A. Amini, D. Westerlund, Evaluation of association constants between drug enantiomers and human alpha 1-acid glycoprotein by applying a partial-filling technique in affinity capillary electrophoresis, Anal. Chem. 70 (1998) 1425–1430.
[41] J. Heintz, M. Hernandez, F.A. Gomez, Use of a partial-filling technique in affinity capillary electrophoresis for determining binding constants of ligands to receptors, J. Chromatogr. A 840 (1999) 261–268.
[42] Y. Zhang, C. Kodama, C. Zurita, F.A. Gomez, On-column ligand synthesis coupled to partial-filling affinity capillary electrophoresis to estimate binding constants of ligands to a receptor, J. Chromatogr. A 928 (2001) 233–241.
[43] J. Kaddis, E. Mito, J. Heintz, A. Plazas, F.A. Gomez, Flow-through partial-filling affinity capillary electrophoresis can estimate binding constants of neutral ligands to receptors via a competitive assay technique, Electrophoresis 24 (2003) 1105–1110.
[44] V. Villareal, J. Kaddis, M. Azad, C. Zurita, I. Silva, L. Hernandez, M. Rudolph, J. Moran, F.A. Gomez, Partial-filling affinity capillary electrophoresis, Anal. Bioanal. Chem. 376 (2003) 822–831.
[45] M. Azad, J. Kaddis, V. Villareal, L. Hernandez, C. Silverio, F.A. Gomez, Affinity capillary electrophoresis to examine receptor–ligand interactions, Methods Mol. Biol. 276 (2004) 153–168.
[46] M. Nilsson, V. Harang, M. Bergström, S. Ohlson, R. Isaksson, G. Johansson, Determination of protein–ligand affinity constants from direct migration time in capillary electrophoresis, Electrophoresis 25 (2004) 1829–1836.
[47] M. Bergström, M. Nilsson, R. Isaksson, I. Rydén, P. Påhlsson, S. Ohlson, Lectin affinity capillary electrophoresis in glycoform analysis applying the partial filling technique, J. Chromatogr. B: Anal. Technol. Biomed. Life Sci. 809 (2004) 323–329.
[48] M. Azad, C. Silverio, Y. Zhang, V. Villareal, F.A. Gomez, On-column synthesis coupled to affinity capillary electrophoresis for the determination of binding constants of peptides to glycopeptide antibiotics, J. Chromatogr. A 1027 (2004) 193–202.
[49] J. Zavaleta, D.B. Chinchilla, A. Ramirez, A. Pao, K. Martinez, S. Nilapwar, J.E. Ladbury, S. Mallik, F.A. Gomez, Partial filling multiple injection affinity capillary electrophoresis (PFMIACE) to estimate binding constants of receptors to ligands, Talanta 71 (2007) 192–201.
[50] R.E. Montes, G. Hanrahan, F.A. Gomez, Use of chemometric methodology in optimizing conditions for competitive binding partial filling affinity capillary electrophoresis, Electrophoresis 29 (2008) 3325–3332.
[51] B.L. Chu, J.M. Lin, Z. Wang, B. Guo, Enantiospecific binding of Rotigotine and its antipode to serum albumins: investigation of binding constants and binding sites by partial-filling ACE, Electrophoresis 30 (2009) 2845–2852.
[52] A.J. Wang, K. Vainikka, J. Witos, L. D'Ulivo, G. Cilpa, P.T. Kovanen, K. Oörni, M. Jauhiainen, M.L. Riekkola, Partial filling affinity capillary electrophoresis with cationic poly(vinylpyrrolidone)-based copolymer coatings for studies on human lipoprotein–steroid interactions, Anal. Biochem. 399 (2010) 93–101.
[53] K. Lipponen, P.W. Stege, G. Cilpa, J. Samuelsson, T. Fornstedt, M.L. Riekkola, Three different approaches for the clarification of the interactions between lipoproteins and chondroitin-6-sulfate, Anal. Chem. 83 (2011) 6040–6046.
[54] Y. Yagi, S. Yamamoto, K. Kakehi, T. Hayakawa, Y. Ohyama, S. Suzuki, Application of partial-filling capillary electrophoresis using lectins and glycosidases for the characterization of oligosaccharides in a therapeutic antibody, Electrophoresis 32 (2011) 2979–2985.
[55] S.L. Diaz, V. Padler-Karavani, D. Ghaderi, N. Hurtado-Ziola, H. Yu, X. Chen, E.C. Brinkman-Van der Linden, A. Varki, N.M. Varki, Sensitive and specific detection of the non-human sialic acid N-glycolylneuraminic acid in human tissues and biotherapeutic products, PLoS One 4 (2009) e4241.
[56] S. Kamoda, R. Ishikawa, K. Kakehi, Capillary electrophoresis with laser-induced fluorescence detection for detailed studies on N-linked oligosaccharide profile of therapeutic recombinant monoclonal antibodies, J. Chromatogr. A 1133 (2006) 332–339.
[57] E. Fukushima, Y. Yagi, S. Yamamoto, Y. Nakatani, K. Kakehi, T. Hayakawa, S. Suzuki, Partial filling affinity capillary electrophoresis using large-volume sample stacking with an electroosmotic flow pump for sensitive profiling of glycoprotein-derived oligosaccharides, J. Chromatogr. A 1246 (2012) 84–89.
[58] N. Suzuki, K.H. Khoo, C.M. Chen, H.C. Chen, Y.C. Lee, N-glycan structures of pigeon IgG: a major serum glycoprotein containing Galalpha1-4 Gal termini, J. Biol. Chem. 278 (2003) 46293–46306.
[59] H. Kalay, M. Ambrosini, P.H. van Berkel, P.W. Parren, Y. van Kooyk, J.J. García Vallejo, Online nanoliquid chromatography–mass spectrometry and nanofluorescence detection for high-resolution quantitative N-glycan analysis, Anal. Biochem. 423 (2012) 153–162.
[60] B.R. Kilgore, A.W. Lucka, R. Patel, B.A. Andrien, S.T. Dhume, Comparability and monitoring immunogenic N-linked oligosaccharides from recombinant monoclonal antibodies from two different cell lines using HPLC with fluorescence detection and mass spectrometry, Methods Mol. Biol. 446 (2008) 333–346.
[61] K.M. Cox, J.D. Sterling, J.T. Regan, J.R. Gasdaska, K.K. Frantz, C.G. Peele, A. Black, D. Passmore, C. Moldovan-Loomis, M. Srinivasan, S. Cuison, P.M. Cardarelli, L.F. Dickey, Glycan optimization of a human monoclonal antibody in the aquatic plant *Lemna minor*, Nat. Biotechnol. 24 (2006) 1591–1597.
[62] D. Liénard, C. Sourrouille, V. Gomord, L. Faye, Pharming and transgenic plants, Biotechnol. Annu. Rev. 13 (2007) 115–147.
[63] A. Triguero, G. Cabrera, L. Royle, D.J. Harvey, P.M. Rudd, R.A. Dwek, M. Bardor, P. Lerouge, J.A. Cremata, Chemical and enzymatic N-glycan release comparison for N-glycan profiling of monoclonal antibodies expressed in plants, Anal. Biochem. 400 (2010) 173–183.
[64] P. Ahmad, M. Ashraf, M. Younis, X. Hu, A. Kumar, N.A. Akram, F. Al-Qurainy, Role of transgenic plants in agriculture and biopharming, Biotechnol. Adv. 30 (2012) 524–540.
[65] M. Tomita, R. Hino, S. Ogawa, M. Iizuka, T. Adachi, K. Shimizu, H. Sotoshiro, K. Yoshizatom, A germline transgenic silkworm that secretes recombinant proteins in the sericin layer of cocoon, Transgenic Res. 16 (2007) 449–465.
[66] M. Iizuka, S. Ogawa, A. Takeuchi, S. Nakakita, Y. Kubo, Y. Miyawaki, J. Hirabayashi, M. Tomita, Production of a recombinant mouse monoclonal antibody in transgenic silkworm cocoons, FEBS J. 276 (2009) 5806–5820.
[67] K. Tatematsu, I. Kobayashi, K. Uchino, H. Sezutsu, T. Iizuka, N. Yonemura, T. Tamura, Construction of a binary transgenic gene expression system for recombinant protein production in the middle silk gland of the silkworm *Bombyx mori*, Transgenic Res. 19 (2010) 473–487.
[68] K. Fötisch, S. Vieths, N- and O-linked oligosaccharides of allergenic glycoproteins, Glycoconjugate J. 18 (2001) 373–390.
[69] V. Gomord, C. Sourrouille, A.C. Fitchette, M. Bardor, S. Pagny, P. Lerouge, L. Faye, Production and glycosylation of plant-made pharmaceuticals: the antibodies as a challenge, Plant Biotechnol. J. 2 (2004) 83–100.
[70] S. Hino, T. Matsubara, A. Urisu, N. Aoki, C. Sato, T. Okajima, D. Nadano, T. Matsuda, Periodate-resistant carbohydrate epitopes recognized by IgG and IgE antibodies from some of the immunized mice and patients with allergy, Biochem. Biophys. Res. Commun. 380 (2009) 632–637.

Stem Cell Research (2012) 8, 300–311

Available online at www.sciencedirect.com

SciVerse ScienceDirect

www.elsevier.com/locate/scr

SHORT REPORT

Promotion of hematopoietic differentiation from mouse induced pluripotent stem cells by transient HoxB4 transduction

Katsuhisa Tashiro [a], Kenji Kawabata [a,b], Miyuki Omori [a,b], Tomoko Yamaguchi [a], Fuminori Sakurai [b], Kazufumi Katayama [b], Takao Hayakawa [c,d], Hiroyuki Mizuguchi [a,b,e,*]

[a] *Laboratory of Stem Cell Regulation, National Institute of Biomedical Innovation, 7-6-8, Saito-Asagi, Ibaraki, Osaka 567-0085, Japan*
[b] *Graduate School of Pharmaceutical Sciences, Osaka University, 1-6, Yamadaoka, Suita, Osaka, 565-0871, Japan*
[c] *Pharmaceutics and Medical Devices Agency, 3-3-2, Kasumigaseki, Chiyoda-Ku, Tokyo 100-0013, Japan*
[d] *Pharmaceutical Research and Technology Institute, Kinki University, 3-4-1, Kowakae, Higashi-Osaka, Osaka 577-8502, Japan*
[e] *The Center for Advanced Medical Engineering and Informatics, Osaka University, 1-6, Yamadaoka, Suita, Osaka, 565-0871, Japan*

Received 25 April 2011; received in revised form 1 September 2011; accepted 5 September 2011
Available online 16 September 2011

Abstract Ectopic expression of HoxB4 in embryonic stem (ES) cells leads to an efficient production of hematopoietic cells, including hematopoietic stem/progenitor cells. Previous studies have utilized a constitutive HoxB4 expression system or tetracycline-regulated HoxB4 expression system to induce hematopoietic cells from ES cells. However, these methods cannot be applied therapeutically due to the risk of transgenes being integrated into the host genome. Here, we report the promotion of hematopoietic differentiation from mouse ES cells and induced pluripotent stem (iPS) cells by transient HoxB4 expression using an adenovirus (Ad) vector. Ad vector could mediate efficient HoxB4 expression in ES cell-derived embryoid bodies (ES-EBs) and iPS-EBs, and its expression was decreased during cultivation, showing that Ad vector transduction was transient. A colony-forming assay revealed that the number of hematopoietic progenitor cells with colony-forming potential in HoxB4-transduced cells was significantly increased in comparison with that in non-transduced cells or LacZ-transduced cells. HoxB4-transduced cells also showed more efficient generation of CD41-, CD45-, or Sca-1-positive cells than control cells. These results indicate that transient, but not constitutive, HoxB4 expression is sufficient to augment the hematopoietic differentiation of ES and iPS cells, and that our method would be useful for clinical applications, such as cell transplantation therapy.

Introduction

Embryonic stem (ES) cells and induced pluripotent stem (iPS) cells, each of which is derived from the inner cell mass of blastocysts and somatic cells by transducing three or four

* Corresponding author at: Laboratory of Biochemistry and Molecular Biology, Graduate School of Pharmaceutical Sciences, Osaka University, 1-6 Yamadaoka, Suita, Osaka 565-0871, Japan. Fax: +81 6 6879 8186.
E-mail address: mizuguch@phs.osaka-u.ac.jp (H. Mizuguchi).

1873-5061/$ - see front matter © 2011 Elsevier B.V. All rights reserved.
doi:10.1016/j.scr.2011.09.001

transcription factors, respectively, can differentiate into various types of cells *in vitro*. They are thus considered as a valuable model to understand the processes involved in the differentiation of lineage-committed cells as well as an unlimited source of cells for therapeutic applications such as hematopoietic stem/progenitor cell (HSPC) transplantation (Evans and Kaufman, 1981; Thomson et al., 1998; Keller, 2005; Takahashi and Yamanaka, 2006; Takahashi et al., 2007).

Differentiation of ES and iPS cells into mature hematopoietic cells, including erythrocytes, myeloid cells, and lymphoid cells, has been performed by embryoid body (EB) formation or coculture with stromal cells (Nakano et al., 1994; Chadwick et al., 2003; Schmitt et al., 2004; Vodyanik et al., 2005). However, the development of an efficient differentiation method for immature hematopoietic cells, including HSPCs, from ES and iPS cells has been challenging. Previously, Daley and his colleagues have shown that enforced expression of HoxB4 in mouse ES cells by a retrovirus vector robustly enhanced the differentiation of ES cells into HSPCs *in vitro*, and these ES cell-derived HSPCs had a long-term reconstitution potential *in vivo* (Kyba et al., 2002; Wang et al., 2005). In addition, constitutive expression of HoxB4 was shown to induce the hematopoietic differentiation from human ES cells (Bowles et al., 2006). These findings indicated that manipulation of HoxB4 expression would be effective for production of HSPCs from ES and iPS cells. However, it is known that long-term constitutive HoxB4 expression in HSPCs has an inhibitory effect on the differentiation of certain hematopoietic lineages, such as lymphoid cells and erythroid cells (Kyba et al., 2002; Pilat et al., 2005), and can lead to a significant risk of leukemogenesis in large animals (Zhang et al., 2008). Although a tetracycline-inducible HoxB4 expression system has been utilized to overcome these unwanted effects, this gene expression system is complex, and cannot be directly applied to therapeutic use. Foreign genes can be integrated into the host chromosome in a stable gene expression system that includes a tetracycline-regulated system, and this could cause an increased risk of cellular transformation (Li et al., 2002; Hacein-Bey-Abina et al., 2003; Williams and Baum, 2004). Therefore, to apply ES cell- and iPS cell-derived HSPCs to clinical medicine, development of a simple and transient HoxB4 transduction method in ES and iPS cells is required.

We have utilized an adenovirus (Ad) vector as a tool for transduction of functional genes into stem cells, because Ad vectors are relatively easy to construct, can be produced at high titers, and mediate efficient and transient gene expression in both dividing and nondividing cells. We have demonstrated that Ad vectors could efficiently transduce a foreign gene in stem cells, including ES and iPS cells (Kawabata et al., 2005; Tashiro et al., 2009, 2010). We also succeeded in promoting the differentiation of osteoblasts, adipocytes, or hepatoblasts from ES and iPS cells by Ad vector-mediated transient transduction of Runx2, PPARγ, or Hex, respectively (Tashiro et al., 2009, 2008; Inamura et al., 2011).

Our data led us to examine whether HSPCs could also be efficiently differentiated from ES and iPS cells by Ad vector-mediated transduction of a HoxB4. In the present study, we investigated whether or not differentiation of HSPCs from mouse ES and iPS cells could be promoted by transient HoxB4 expression. Our results showed that Ad vector-mediated transient HoxB4 expression in mouse ES and iPS cells are sufficient to augment the differentiation of hematopoietic cells, including HSPCs, from mouse ES and iPS cells. This result indicates that an Ad vector-mediated transient gene expression system would be a powerful and safe tool to induce hematopoietic differentiation from mouse ES and iPS cells.

Results

Transduction with Ad vectors in ES-EBs or iPS-EBs

A previous study using a tetracycline-inducible HoxB4 expression system showed that hematopoietic stem/progenitor cells (HSPCs) were generated by induction of HoxB4 expression in ES cell-derived embryoid bodies (ES-EBs) from day 4 to day 6 of differentiation (Kyba et al., 2002), suggesting that HoxB4 expression within this time range would be effective for induction of hematopoietic cells. In addition, $CD41^+c\text{-}kit^+$ cells in EBs are reported to be early hematopoietic progenitor cells (Mitjavila-Garcia et al., 2002; Mikkola et al., 2003). Thus, we planned to transduce HoxB4 in total cells derived from ES- or iPS-EBs on day 5 of differentiation or in $CD41^+c\text{-}kit^+$ cells derived from ES- or iPS-EBs on day 6. We initially investigated the expression of coxsackievirus and adenovirus receptor (CAR) in ES-EB- or iPS-EB-derived cells, because CAR was indispensable for transduction of an exogenous gene using Ad vector (Bergelson et al., 1997; Tomko et al., 1997). Flow cytometric analysis showed the expression of CAR in ES-EB- and iPS-EB-derived total cells and $CD41^+c\text{-}kit^+$ cells, although the expression levels of CAR in $CD41^+c\text{-}kit^+$ cells were decreased in comparison with that in total cells (Figs. 1a and b). These results indicate that ES-EB- and iPS-EB-derived total cells and $CD41^+c\text{-}kit^+$ cells could be transduced with Ad vectors. We also observed the expression of green fluorescent protein (GFP) in iPS-EB-derived total cells. Because the mouse iPS cells used in this study express GFP under the control of Nanog promoter (Okita et al., 2007), the existence of GFP-positive cells showed that undifferentiated iPS cells would still be present in iPS-EB-derived total cells.

We next examined the transduction efficiency in EB-derived total cells or EB-derived $CD41^+c\text{-}kit^+$ cells using DsRed- or GFP-expressing Ad vectors, respectively. After transduction with Ad-DsRed or Ad-GFP at 3000 vector particles (VPs)/cell, the cells were cultured with the hematopoietic cytokines for 2 days. The results showed that, at 3000 VPs/cell, approximately 60% or 40% of the EB-derived total cells or EB-derived $CD41^+c\text{-}kit^+$ cells, respectively, expressed transgenes (Figs. 1c and d). Although the number of transgene-expressing cells was increased in the case of transduction with Ad vectors at 10,000 VPs/cell, the number of viable cells was markedly reduced (data not shown). Therefore, we decided to use Ad vectors at 3000 VPs/cell for transducing human HoxB4 (hHoxB4) into ES-EBs and iPS-EBs. RT-PCR analysis on day 3 after transduction with Ad-hHoxB4 into EB-derived total cells showed an elevation of hHoxB4 mRNA expression in hHoxB4-transduced cells, while neither non-transduced cells nor LacZ-transduced cells showed hHoxB4 expression (Fig. 1e). Importantly, the expression level of hHoxB4 in the cells was markedly decreased on day 6 after Ad

transduction. This result showed that the ES-EB- or iPS-EB-derived cells could express transgenes by Ad vectors, and that Ad vector mediated the transient transgene expression in these cells.

Transient HoxB4 expression augments the generation of hematopoietic cells from mouse ES and iPS cells

To induce and expand the hematopoietic cells from the iPS cell line 38C2, EB-derived total cells were plated and cultured on OP9 stromal cells with the hematopoietic cytokines. On day 10 after plating on OP9 cells, the number of 38C2-derived hematopoietic cells in LacZ-transduced cells was similar to that in non-transduced cells. On the other hand, transient transduction of HoxB4 with Ad-hHoxB4 resulted in a significant increase in the number of hematopoietic cells compared with non-transduced cells or LacZ-transduced cells (Fig. 2a, middle). Likewise, an increase in the hematopoietic cell number by Ad vector-mediated hHoxB4 transduction was also observed in ES cell derived-hematopoietic cells or the other iPS line 20D17-derived hematopoietic cells (Fig. 2a, left and right). Additionally, ES-EB- or iPS-EB-derived $CD41^+c\text{-}kit^+$ cells, which were transiently transduced with hHoxB4, could proliferate on OP9 stromal cells for over 20 days (Fig. 2b). This result is mostly in agreement with the previous report that ES cell-derived hematopoietic cells stably expressing HoxB4 had a growth advantage in the presence of hematopoietic cytokines (Pilat et al., 2005). Transient, but not stable, HoxB4 expression in ES-EB- or iPS-EB-derived cells would be sufficient to augment the generation of hematopoietic cells from ES and iPS cells.

We next investigated the surface antigen expression in non-transduced cells, LacZ-transduced cells, or hHoxB4-transduced cells after expansion on OP9 stromal cells. Flow cytometric analysis revealed an increase of CD45 and CD41 expressions in HoxB4-transduced cells, compared with non-transduced cells and LacZ-transduced cells (Figs. 3a and b). CD45 is known as a marker of hematopoietic cells. In both *in vitro* ES cell differentiation and a developing mouse embryo, the expression of CD45 was developmentally controlled, and CD45 expression was observed on hematopoietic cells after expression of CD41 (Mitjavila-Garcia et al., 2002; Mikkola et al., 2003). Thus, a higher percentage of $CD45^+$ cells in HoxB4-transduced cells would be due, at least in part, to an increase of CD41 expression in HoxB4-transduced cells relative to non-transduced cells and LacZ-transduced cells. We also found a significant elevation of Sca-1 in hHoxB4-transduced cells (Figs. 3a and b). Sca-1 is expressed in fetal and adult HSPCs (Arai et al., 2004; McKinney-Freeman et al., 2009), although Sca-1 expression was observed in other types of cells. Therefore, our data suggest that immature hematopoietic cells would be generated in hHoxB4-transduced cells more efficiently than in non-transduced cells or LacZ-transduced cells.

In parallel with the flow cytometric analysis, we also analyzed the expression levels of hematopoietic marker genes in iPS cell-derived hematopoietic cells by RT-PCR (Fig. 3c). The expression levels of marker genes in LacZ-transduced cells were mostly equal to those in non-transduced cells. In contrast, among the genes we assayed, the expression levels of *Gata-1*, *c-myb*, and *Cxcr4* mRNA were slightly but significantly up-regulated in hHoxB4-transduced cells. GATA-1 reflects early hematopoietic development, whereas c-Myb is a marker of definitive hematopoiesis (Godin and Cumano, 2002). Increased expression of these genes in HoxB4-transduced cells suggests that transient hHoxB4 expression promotes the production of both primitive and definitive hematopoietic progenitor cells from mouse ES and iPS cells. We could not detect the hHoxB4 mRNA expression in Ad-hHoxB4-transduced cells, confirming the transient hHoxB4 expression by Ad vectors (Fig. 3c).

HoxB4 expression enhances development of hematopoietic progenitor cells from mouse ES and iPS cells

To examine whether hematopoietic immature cells with hematopoietic colony-forming potential could be generated from ES and iPS cells, ES cell-derived hematopoietic cells and iPS cell-derived hematopoietic cells, both of which were cultured on OP9 stromal cells for 10 days, were plated and cultured in methylcellulose-containing media with hematopoietic cytokines. Without Ad transduction, the number of total hematopoietic colonies in the iPS cell line 38C2 was five times as high as that in ES cells, whereas another iPS cell line, 20D17, had nearly the same hematopoietic differentiation potential as ES cells (Fig. 4a). These results indicate that there is a difference in hematopoietic differentiation potential among iPS cell lines.

We next examined the hematopoietic colony potential in LacZ-transduced cells or HoxB4-transduced cells. The colony assay revealed a significant increase in the number of total hematopoietic colonies in hHoxB4-transduced cells compared with control cells, whereas there was no significant difference in the number of hematopoietic colonies between

Figure 1 Transduction with Ad vectors in ES-EB- or iPS-EB-derived cells. (a, b) The expression levels of CAR, a primary receptor for Ad, in ES-EB- or iPS-EB-derived total cells (a) or $CD41^+c\text{-}kit^+$ cells (b) were detected with anti-mouse CAR monoclonal antibody by flow cytometric analysis. As a negative control, the cells were incubated with an irrelevant antibody. Data shown are from one representative experiment of three performed. (c, d) EB-derived total cells (c) or $CD41^+c\text{-}kit^+$ cells (d), purified by FACS (Supplemental Fig. 1), were transduced with Ad-DsRed or Ad-GFP for 1.5 h, and transgene-expressing cells were then analyzed by flow cytometry. Because $CD41^+c\text{-}kit^+$ cells do not express GFP (Fig. 1b), Ad-GFP was used for transduction into $CD41^+c\text{-}kit^+$ cells. Similar results were obtained in three independent experiments. (e) The expression level of human HoxB4 mRNA in the cells was examined by conventional RT-PCR on days 3 and 6 after transduction with Ad-hHoxB4 at 3000 VPs/cell into EB-derived total cells. Abbreviations: ES, embryonic stem; iPS, induced pluripotent stem; mCAR, mouse coxsackievirus and adenovirus receptor; GFP, green fluorescent protein; Cont., control.; VP, vector particle; RT, reverse transcription; GAPDH, glyceraldehyde-3-phosphate dehydrogenase.Transduction with Ad vectors

non-transduced cells and LacZ-transduced cells (Fig. 4a). Note that the number of the most immature multipotent progenitor cells, CFU-GEMM/CFU-Mix, in hHoxB4-transduced cells was approximately seven times as great as that in non-transduced cells or LacZ-transduced cells, and that large CFU-Mix colonies were more frequently observed in hHoxB4-transduced cells than control cells (Fig. 4b and data not shown). A colony assay after culturing on OP9 stromal cells for 20 days also revealed that much number of myeloid (CFU-G, M, and GM) colonies and CFU-Mix colonies were observed by transient hHoxB4 transduction (Figs. 4c and d). Thus, our data clearly showed that Ad vector-mediated transient hHoxB4 expression

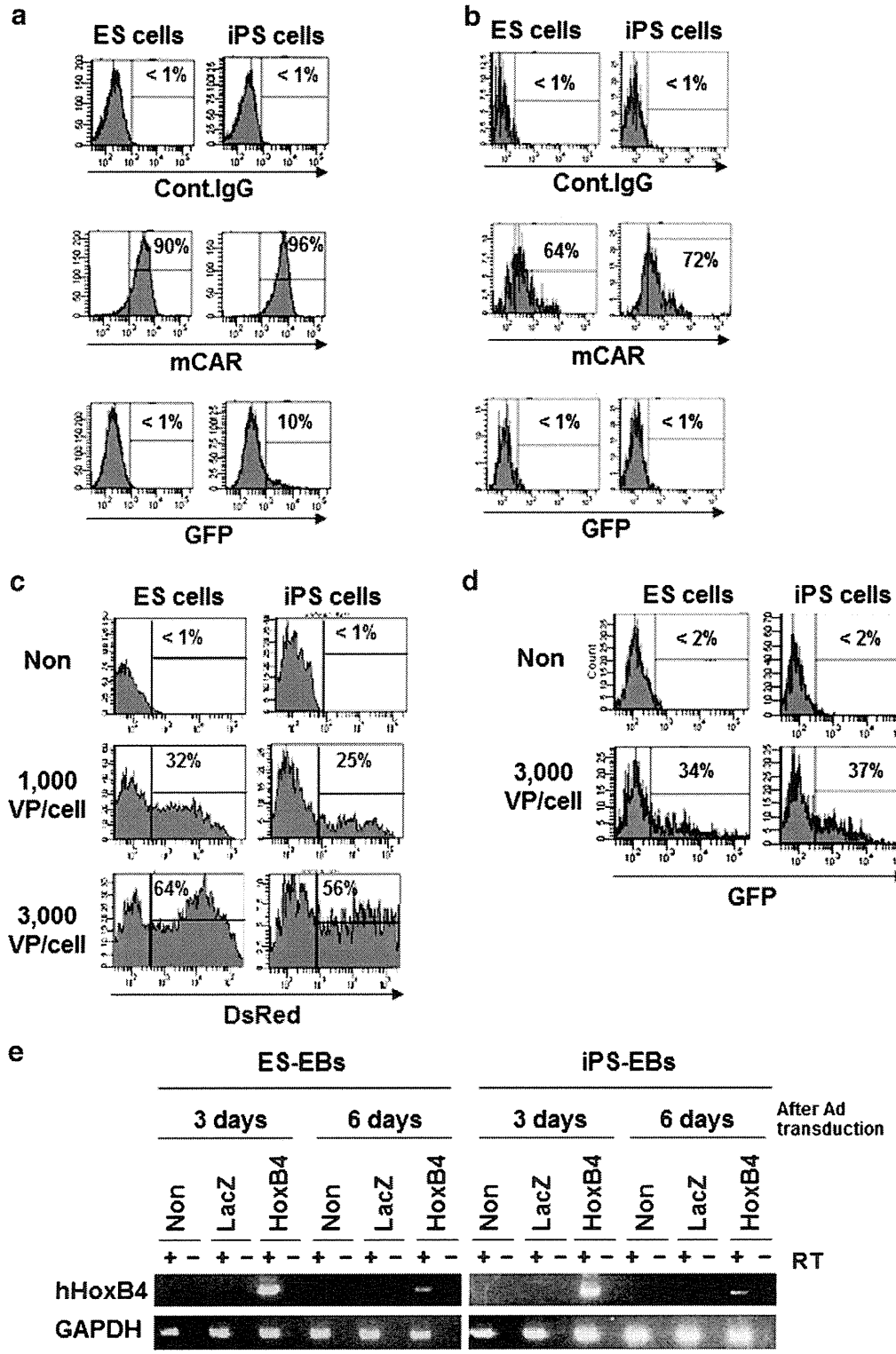

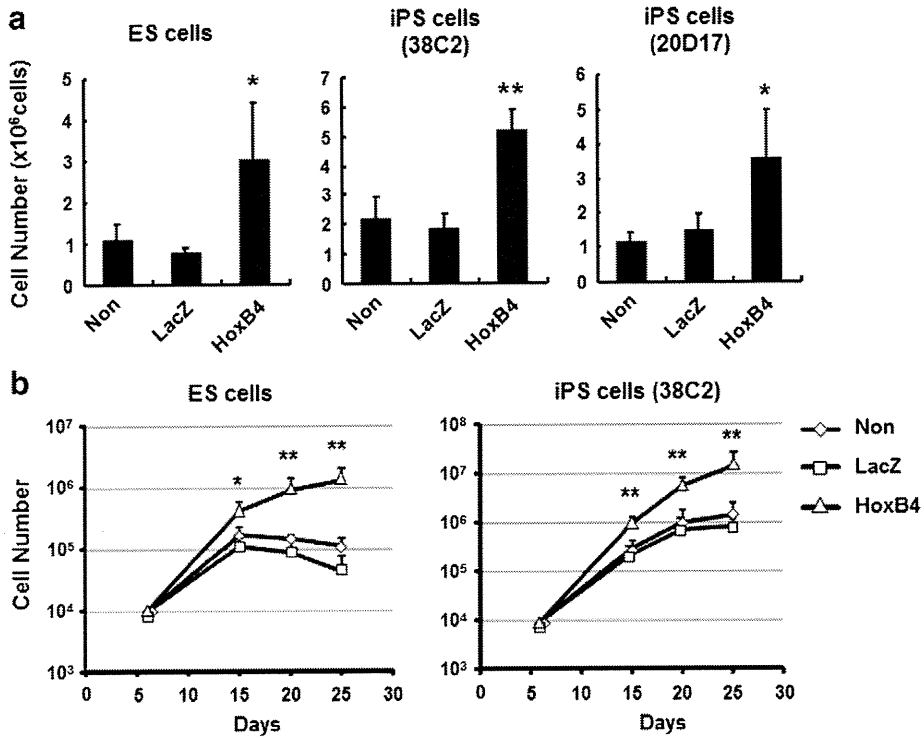

Figure 2 The number of ES cell- or iPS cell-derived hematopoietic cells was significantly increased in Ad-hHoxB4-transduced cells. (a, b) ES-EB- or iPS-EB-derived total cells (a) or CD41$^+$c-kit$^+$ cells (b) were transduced with Ad-LacZ or Ad-hHoxB4 at 3000 VPs/cell for 1.5 h, and the cells were then plated on OP9 feeder cells. As a control, non-transduced cells were also plated on OP9 cells. After culturing on OP9 feeders with the hematopoietic cytokines for 10 days (a) or 20 days (b), the number of hematopoietic cells per 2 wells of a 6-well plate was counted. (a) Left, ES cells; middle, iPS cell line 38C2; right, iPS cell line 20D17. Results shown were the mean of four independent experiments with indicated standard deviations. * $p<0.05$, ** $p<0.01$ as compared with non-transduced or Ad-LacZ-transduced cells.

enhances the differentiation of hematopoietic immature cells, including HSPCs, from mouse ES and iPS cells.

Discussion

Previous studies have shown that enforced expression of HoxB4 is an effective strategy for hematopoietic differentiation from both mouse and human ES cells (Kyba et al., 2002; Bowles et al., 2006; Pilat et al., 2005; Schiedlmeier et al., 2007). These studies usually used recombinant ES cells, such as ES cells constitutively expressing HoxB4 (Pilat et al., 2005) or ES cells containing a tetracycline (Tet)-inducible HoxB4 expression system (Kyba et al., 2002), to induce hematopoietic cells. However, this expression system might raise clinical concerns, including the risk of oncogenesis due to integration of transgenes into host genomes. In the present study, we showed that Ad vector-mediated transient hHoxB4 expression in mouse ES-EB- or iPS-EB-derived cells could result in an efficient production of hematopoietic cells, including HSPCs with a hematopoietic colony-forming ability, from mouse ES and iPS cells (Figs. 2, 3, and 4). Our data obtained in this report are largely consistent with previous reports (Kyba et al., 2002) in which HSPCs were generated by using ES cells containing the Tet-regulated HoxB4 expression cassette. Therefore, a transient HoxB4 expression system using an Ad vector, instead of a Tet-inducible HoxB4 expression system, would contribute to safer clinical applications of ES or iPS cell-derived hematopoietic cells.

Conventional Ad vector is known to infect the cells through an entry receptor, CAR, on the cellular surface (Bergelson et al., 1997; Tomko et al., 1997). Previously, we showed that undifferentiated ES and iPS cells expressed CAR, and conventional Ad vector could easily transduce a foreign gene in more than 90% of the undifferentiated ES and iPS cells at 3000 VPs/cell (Kawabata et al., 2005; Tashiro et al., 2009). Like undifferentiated ES and iPS cells, we could detect the CAR expression in more than 90% or 70% of EB-derived total cells or EB-derived CD41$^+$c-kit$^+$ cells, respectively (Figs. 1a and b). However, the transduction efficiency in EB-derived total cells or CD41$^+$c-kit$^+$ cells was only 60% or 40%, respectively, of the cells at most (Figs. 1c and d). Although we are not certain why transgene expression was not observed in all of CAR$^+$ EB-derived cells, it is possible that the promoter might not have worked in all of the cells because the EB-derived total cells and CD41$^+$c-kit$^+$ cells were heterogeneous, unlike in the case of undifferentiated ES and iPS cells. It is also possible that the Ad binding site of CAR might be disrupted by trypsin treatment during the preparation of the EB-derived cells (Carson, 2000). Because the development of efficient transduction methods in EB-derived cells is considered to be a powerful tool to promote the hematopoietic differentiation from ES and iPS cells, further improvement of the transduction conditions will be needed.

We found a difference in the hematopoietic differentiation potential among mouse iPS cell lines (Fig. 4). Consistent with our data, Kulkeaw et al. showed a difference in the hematopoietic differentiation capacity among six iPS cell lines (Kulkeaw et al., 2010). In addition, recent studies have reported that iPS cells leave an epigenetic memory of

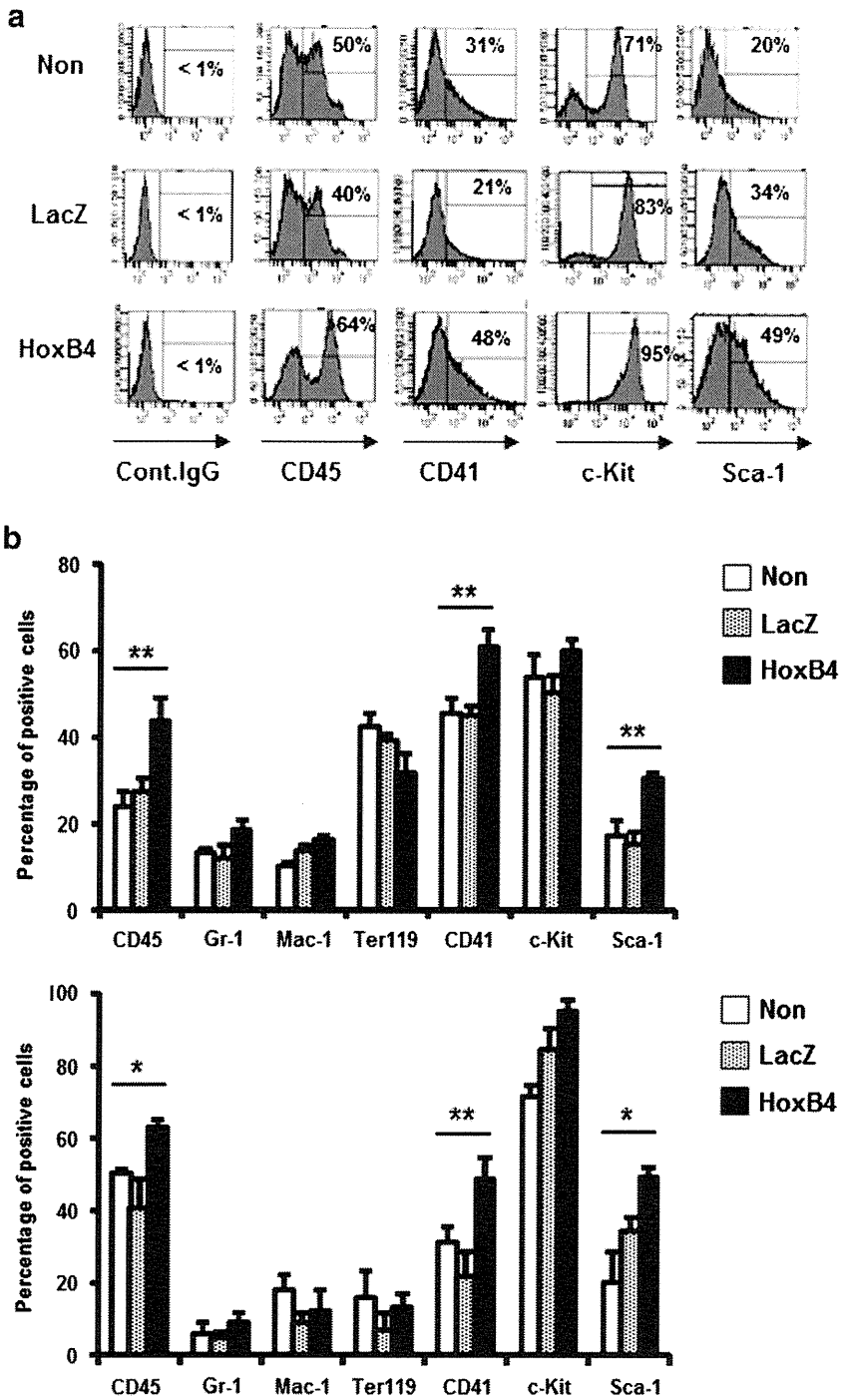

Figure 3 Expression of surface antigen and hematopoietic marker genes in mouse ES cell- or iPS cell-derived cells. (a, b) ES cell- or iPS cell line 38C2-derived cells were reacted with each antibody, and were then subjected to flow cytometric analysis. (a) Representative data from iPS cell line 38C2 are shown. (b) Percentage of each antigen positive cells in ES cell-derived cells (upper) or iPS cell-derived cells (lower) is shown. The data expressed the mean of three independent experiments with indicated standard deviations. * $p<0.05$, ** $p<0.01$ as compared with non-transduced or Ad-LacZ-transduced cells. (c) Total RNA was extracted from undifferentiated iPS cells (Day 0), iPS-EB (Day 5), iPS cells-derived hematopoietic cells (day 15), OP9 stromal cells, and MEF feeder, and semi-quantitative PCR (left) or quantitative real-time PCR (right) was then carried out as described in the Materials and methods. The data expressed the mean of three independent experiments with indicated standard deviations. * $p<0.05$, ** $p<0.01$ as compared with non-transduced or Ad-LacZ-transduced cells. Abbreviation: EBs, embryoid bodies; MEF, mouse embryonic fibroblast; GATA, GATA-binding protein.

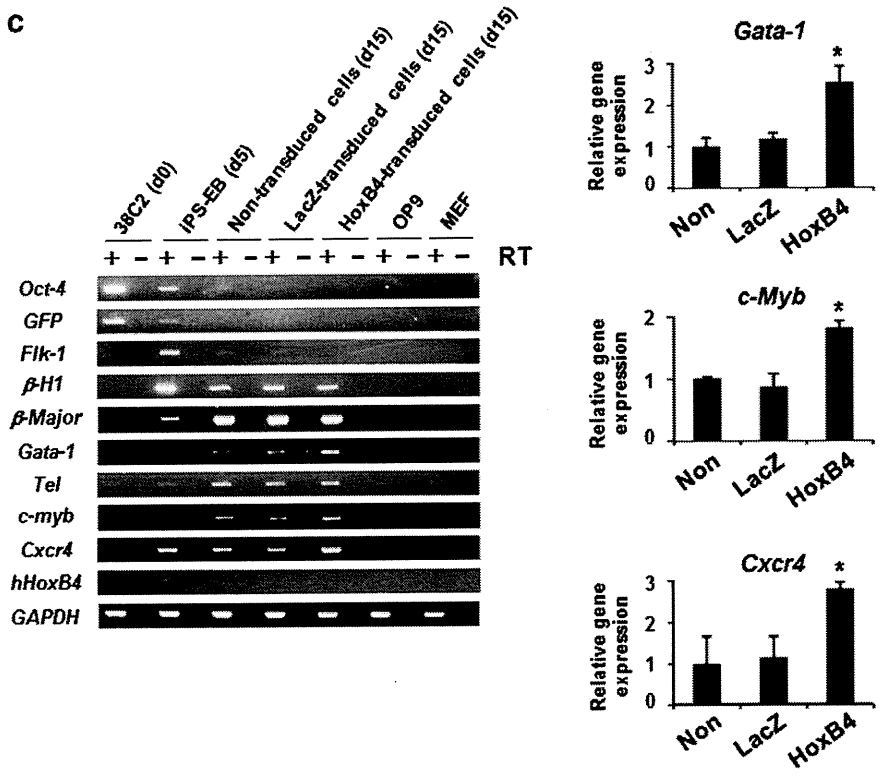

Figure 3 (*continued*).

their cellular origin, and this memory influences their functional properties, including *in vitro* differentiation (Kim et al., 2010; Polo et al., 2010). Thus, these reports indicate that, in order to obtain a large number of HSPCs from iPS cells, it is necessary to choose an appropriate iPS cell line, such as HSPC-derived iPS cells (Okabe et al., 2009). Importantly, using mouse embryonic fibroblast-derived iPS cells (38C2 and 20D17), we showed that the use of transient hHoxB4 transduction in iPS-EB-derived cells achieved more effective differentiation into HSPCs than the use of non-transduced cells (Fig. 4). Our method therefore should be efficient for the production of HSPCs from any iPS cell line.

An important but unsolved question in this study is whether ES cell-derived hematopoietic cells and iPS cell-derived hematopoietic cells transduced with Ad-hHoxB4 have long-term hematopoietic reconstitution potential *in vivo*. Recent studies have demonstrated that some surface antigen expressions were different between bone marrow-derived HSPCs and ES cell-derived HSPCs, and that $CD41^+$ cells had long-term repopulation ability in ES cell-derived HSPCs (McKinney-Freeman et al., 2009; Matsumoto et al., 2009). Our flow cytometric analysis revealed an increase of $CD41^+$ cells in hHoxB4-transduced cells compared with non-transduced cells and LacZ-transduced cells (Fig. 3b). We also showed that Ad-hHoxB4-transduced cells could proliferate on OP9 stromal cells more efficiently than control cells (Fig. 2). Thus, these results suggest that immature hematopoietic cells were generated by transient hHoxB4 transduction, and that hHoxB4-transduced cells might have reconstitution potential *in vivo*. This *in vivo* transplantation analysis is now on-going in our laboratory.

In the present study, we succeeded in the promotion of hematopoietic differentiation from mouse ES and iPS cells by Ad vector-mediated hHoxB4 transduction. Ad vector transduction can avoid the integration of transgene into host genomes, and multiple genes can be transduced by Ad vectors in an appropriate differentiation period. Thus, an even more efficient protocol for hematopoietic differentiation from ES and iPS cells could likely be established by co-transduction of HoxB4 and other genes involved in the hematopoiesis, such as Cdx4 (Wang et al., 2005) and Scl/Tal1 (Kurita et al., 2006), using Ad vectors. Taken together, our results show that Ad vector-mediated transient gene expression is valuable tool to induce hematopoietic cell from ES and iPS cells, and this strategy would be applicable to safe therapeutic applications, such as HSPC transplantation.

Materials and methods

Antibodies

The following primary monoclonal antibodies (Abs), conjugated with fluorescein isothiocyanate (FITC), phycoerythrin (PE), allophycocyanin (APC), or PE-Cy7, were used for flow cytometric analysis: anti-CD45 (30-F11, eBioscience, San Diego, CA), anti-CD11b (M1/70, eBioscience), anti-Sca-1 (D7, eBioscience), anti-Ter-119 (Ter-119, eBioscience), anti-Gr-1 (RB6-8C5, eBioscience), anti-c-Kit (ACK2 or 2B8, eBioscience), anti-CD41 (MWReg30, BD Bioscience San Jose, CA). Purified rat anti-coxsackievirus and adenovirus receptor (CAR) was kindly provided from Dr. T. Imai (KAN Research Institute, Hyogo, Japan). For detection of CAR, the PE-conjugated donkey anti-rat IgG (Jackson ImmunoResearch Laboratories, West

Grove, PA) or DyLight649-conjugated goat anti-rat IgG (BioLegend, San Diego, CA) was used as secondary Abs.

Cell cultures

The mouse ES cell line E14 and two mouse iPS cell lines, 38C2 and 20D17, both of which were generated by Yamanaka and his colleagues (Okita et al., 2007), were used in this study. 38C2 was kindly provided by Dr. S. Yamanaka (Kyoto University, Kyoto, Japan), and 20D17 was purchased from Riken Bioresource Center (Tsukuba, Japan). In the present study, we mainly used 38C2 iPS cells except where otherwise indicated. Mouse ES and iPS cells were cultured in leukemia inhibitory factor-containing medium on a feeder layer of mitomycin C-inactivated mouse embryonic fibroblasts (MEF) as described previously (Tashiro et al., 2009). OP9 stromal cells were cultured in α-minimum essential medium (αMEM: Sigma, St. Louis, MO) supplemented with 20% fetal bovine serum (FBS), 2 mM L-glutamine (Invitrogen, Carlsbad, CA), and non-essential amino acid (Invitrogen).

Ad vectors

Ad vectors were constructed by an improved *in vitro* ligation method (Mizuguchi and Kay, 1998, 1999). The shuttle

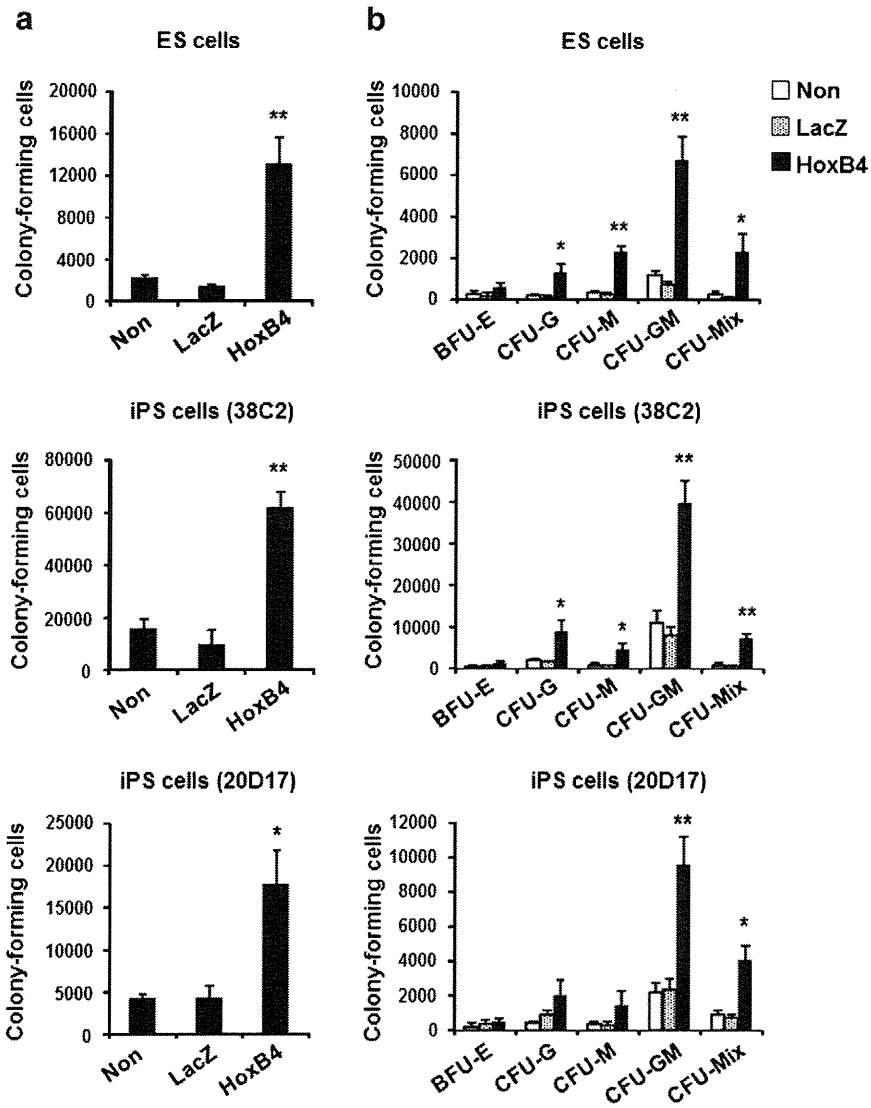

Figure 4 Significant increase of hematopoietic colony-forming cells in Ad-HoxB4-transduced hematopoietic cells. After ES-EB- or iPS-EB-derived cells were transduced with Ad-LacZ or Ad-hHoxB4, hematopoietic cells were generated by co-culturing with OP9 cells in the presence of hematopoietic cytokines for 10 days (a, b) or 20 days (c, d). A colony-forming assay was performed using methylcellulose medium, and the number of hematopoietic colonies was then counted under light microscopy. The number of total colonies (a, c) or subdivided colonies by morphological subtype (BFU-E, CFU-G, CFU-M, CFU-GM, and CFU-Mix) (b, d) generated from ES cells (E14) or iPS cells (38C2 and 20D17) was shown. Colony number was normalized to total number of the cells. Results shown were the mean of three (c, d) or four (a, b) independent experiments with indicated standard deviations. * $p<0.05$, ** $p<0.01$ as compared with non-transduced or Ad-LacZ-transduced cells. Abbreviation: BFU-E, burst-forming unit; CFU-G, colony-forming unit-granulocyte; CFU-M, CFU-monocyte; CFU-GM, CFU-granulocyte, monocyte; CFU-GEMM/CFU-Mix, CFU-granulocyte, erythrocyte, monocyte, megakryocyte.

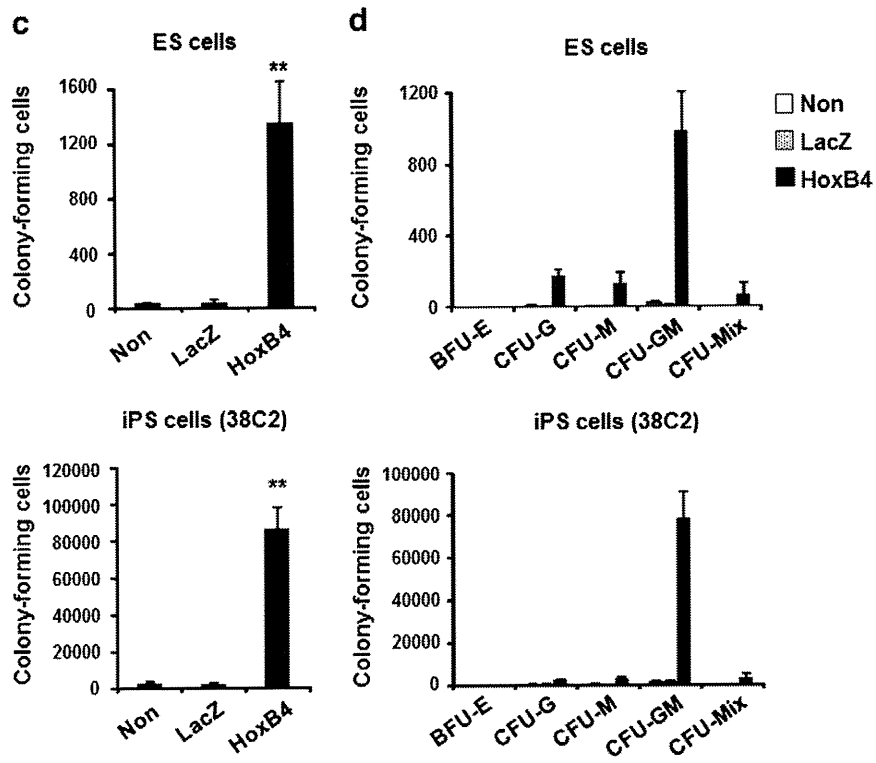

Figure 4 (*continued*).

plasmid pHMCA5, which contains the CMV enhancer/β-actin promoter with β-actin intron (CA) promoter (a kind gift from Dr. J. Miyazaki, Osaka University, Osaka, Japan) (Niwa et al., 1991), was previously constructed (Kawabata et al., 2005). The human HoxB4 (hHoxB4)-expressing plasmid, pHMCA-hHoxB4, and DsRed-expressing plasmid, pHMCA-DsRed, were generated by inserting a hHoxB4 cDNA (a kindly gift from Dr. S. Karlsson, Lund University Hospital, Lund, Sweden) and a DsRed cDNA (Clontech, Mountain View, CA), respectively, into pHMCA5. pHMCA-hHoxB4 or pHMCA-DsRed were digested with I-*Ceu*I/PI-*Sce*I and ligated into I-*Ceu*I/PI-*Sce*I-digested pAdHM4 (Mizuguchi and Kay, 1998), resulting in pAd-hHoxB4 or pAd-DsRed, respectively. Ad-hHoxB4 and Ad-DsRed were generated and purified as described previously (Tashiro et al., 2008). The CA promoter-driven β-galactosidase (LacZ)-expressing Ad vector, Ad-LacZ, and the CA promoter-driven GFP-expressing Ad vector, Ad-CA-GFP, were generated previously (Tashiro et al., 2008). The vector particle (VP) titer was determined by using a spectrophotometrical method (Maizel et al., 1968).

In vitro differentiation

Prior to embryoid body (EB) formation, mouse ES or iPS cells were suspended in differentiation medium (Dulbecco's modified Eagle's medium (Wako, Osaka, Japan) containing 15% FBS, 0.1 mM 2-mercaptoethanol (Nacalai tesque, Kyoto, Japan), 1×non-essential amino acid (Specialty Media, Inc.), 1×nucleosides (Specialty Media, Inc.), 2 mM L-glutamine (Invitrogen), and penicillin/streptomycin (Invitrogen)) and cultured on a culture dish at 37 °C for 45 min to remove MEF layers. Mouse ES cell- or iPS cell-derived EBs (ES-EBs or iPS-EBs, respectively) were generated by culturing ES or iPS cells on a round-bottom low cell binding 96-well plate (Lipidure-coat plate; Nunc) at 1×10^3 cells per well. ES-EBs or iPS-EBs were collected on day 5, and a single cell suspension was prepared by trypsin/EDTA treatment (Invitrogen) at 37 °C for 2 min. ES-EB- or iPS-EB-derived $CD41^+c\text{-}kit^+$ cells were sorted by FACSAria (BD Bioscience). The purity of the $CD41^+c\text{-}kit^+$ cells was greater than 90% based on flow cytometric analysis (Supplemental Fig. 1). Cells were then transduced with an Ad vector at 3000 vector particles (VPs)/cell for 1.5 h in a 15 ml tube. After transduction, total cells (2×10^5) or $CD41^+c\text{-}kit^+$ cells (1×10^4) were cultured on OP9 feeder cells in a well of a 6-well plate in αMEM supplemented with 20% FBS, 2 mM L-glutamine, non-essential amino acid, 0.05 mM 2-mercaptoethanol, and hematopoietic cytokines (50 ng/ml mouse stem cell factor (SCF), 50 ng/ml human Flt-3 ligand (Flt-3L), 20 ng/ml thrombopoietin (TPO), 5 ng/ml mouse interleukin (IL)-3, and 5 ng/ml human IL-6 (all from Peprotec, Rocky Hill, NJ)). After culturing with OP9 stromal cells, both non-adherent hematopoietic cells and adherent hematopoietic cells were collected as follows. The non-adherent hematopoietic cells were collected by pipetting and were transferred to 15 ml tubes. The adherent hematopoietic cells were harvested with the use of trypsin/EDTA, and then incubated in a tissue culture dish for 30 min to eliminate the OP9 cells. Floating cells were collected as hematopoietic cells and transferred to the same 15 ml tubes. These hematopoietic cells were kept on ice for further analysis.

Flow cytometry

Cells (1×10^5 to 5×10^5) were incubated with monoclonal Abs at 4 °C for 30 min and washed twice with staining buffer